TRIBHUVAN UNIVERSITY

INSTITUTE OF ENGINEERING

PULCHOWK CAMPUS

THESIS NO: M-89-MSMDE-2023-2025

Free Vibration Analysis of Circular Tapered Cantilever Microbeams

by

Dhan Bahadur Saud

A THESIS SUBMITTED TO THE DEPARTMENT OF MECHANICAL AND AEROSPACE ENGINEERING IN PARTIAL FULFILLMENT OF THE REQUIREMENTS FOR THE DEGREE OF MASTER OF SCIENCE IN MECHANICAL SYSTEMS DESIGN AND ENGINEERING

DEPARTMENT OF MECHANICAL AND AEROSPACE ENGINEERING

LALITPUR, NEPAL

APRIL, 2025

TRIBHUVAN UNIVERSITY

INSTITUTE OF ENGINEERING

PULCHOWK CAMPUS

DEPARTMENT OF MECHANICAL AND AEROSPACE ENGINEERING

The undersigned certify that they have read, and recommended to the Institute of Engineering for acceptance, a thesis entitled **"Free Vibration Analysis of circular tapered cantilever microbeam"** submitted by **Dhan Bahadur Saud (079msmde006)** in partial fulfillment of the requirements for the degree of Master of Science in Mechanical Systems Design and Engineering.

Supervisor: Prof. Dr. Mahesh Chandra Luintel
Department of Mechanical and Aerospace Engineering,
Pulchowk Campus

Supervisor: Asst. Prof. Laxman Motra
Department of Mechanical and Aerospace Engineering,
Pulchowk Campus

External Examiner: Asst. Prof. Manoj Adhikari
Department of Automobile and Mechanical Engineering,
Thapathali Campus

Committee Chairperson: Asst. Prof. Dr. Sudip Bhattrai
Head of the Department
Department of Mechanical and Aerospace Engineering,
Pulchowk Campus

Tribhuvan University
Institute of Engineering
Department of Mechanical and Aerospace Engineering
Pulchowk Campus

Date: April 7,2025

ABSTRACT

In micro-electromechanical systems (MEMS), based on cantilever microbeams have been widely used in various sensor application. Most research has focused on tapered microbeams with rectangular cross-sections, while circular tapered cantilever microbeams remain relatively unexplored. This study examines the free vibration analysis of a tapered circular cantilever micro-beam with and without an attached mass. A mathematical model is developed using the assumed mode method and solved analytically. The analytical results are validated through simulation on Ansys workbench 2019 R3. The effect of different tapering ratios on their natural frequency, modal mass, and stiffness of microbeams has been analyzed analytically, and natural frequency and mode shape have been investigated by using both analytical and simulation. In this research we found that for beams without an attached mass, the deviation between analytical and simulation natural frequencies is less than 9.3%. With an attached mass, deviations increase to a maximum of 14.3%. As increase in the tapering ratio results in a higher natural frequency due to a reduction in mass distribution and an increase in stiffness.

ACKNOWLEDGMENTS

I would like to sincerely thank my thesis Supervisors, Prof. Dr. Mahesh Chandra Luintel, and assistant Prof. Laxman Motra for their unwavering support, motivation, and valuable insights throughout this study. Their expertise and assistance were essential to finishing the work. In addition, I want to sincerely thank the Department of Mechanical and Aerospace Engineering, Pulchowk Campus, Institute of Engineering for giving me the opportunity to complete the thesis work of Master of Science in Mechanical Systems Design and Engineering.

I am also thankful towards Prof. Dr. Laxman Paudel, Programme Coordinator, Mechanical System Design and Engineering and Asst. Prof. Dr. Sudip Bhattrai, Head of Department, Department of Mechanical and Aerospace Engineering for his constant encouragement and words of wisdom.

I would also like to acknowledge to my colleagues Er. Ghanshyam Aryal, Er. Ayush Bhatta and senior Er. Salim Maharjan, Department of Mechanical Engineering, Pulchowk Campus for supporting me by all means. Lastly, I would also like to express my sincere appreciation to all my dear friends and family for their constant support and care amid which this thesis work is brought into fruition.

TABLE OF CONTENTS

LIST OF FIGURES

LIST OF TABLES

LIST OF SYMBOLS

L	Length of the cantilever microbeam
x	The spatial coordinate along the beam, with x = 0 at the clamped end and x = L at the free end
α	The tapering parameter, it defines the variation in the beam's radius so that the radius at the free end is given by R(L) = αL.
R_0	Radius at the fixed end of the tapered microbeam
R_f	Radius at the free end of the tapered microbeam
R_x	The radius of the beam's cross-section at any position x
h(x)	Thickness of the microbeam as a function of length
A(x)	Cross-sectional area of the beam at position x
I(x)	Area moment of inertia at position x
ρ	Density of the beam material
M	Attached mass at the free end
E	Young's modulus of the material
G	Shear modulus
ν	Poisson's ratio
ω	Natural frequency of vibration
ω_n	n^{th} natural frequency
V(x)	Shear force at position x
$W(x, t)$	Transverse displacement of the beam
M(x)	Bending moment at position x
k	Stiffness parameter
θ(x)	Slope of the beam at position x
$w(0, t)$	Zero displacement at fixed end
$\frac{dw}{dt}$	Zero slope at fixed end
$\emptyset(x)$	Mode shape function of the beam
β	Mass ratio of attached mass to beam mass
k_i	Modal stiffness matrix
m_i	Modal mass matrix
T_b	The Kinetic energy of the beam
T_m	The Kinetic energy of the attached mass at the free end (x = L

T	Total kinetic energy of the system
V	Strain (potential) energy of the beam
L	Lagrangian Functional): Difference between the kinetic and strain energies, L = T – V.
$\delta(x - L)$	Dirac delta function, used to model the concentrated mass at the free end

LIST OF ABBREVIATIONS

FEM	Finite Element Method
DOF	Degree of Freedom
CBM	Circular Tapered Beam Model
MEMS	Microelectromechanical Systems
NEMS	Nanoelectromechanical Systems
CFD	Computational Fluid Dynamics
ANSYS	Analysis System (Software)
FEA	Finite Element Analysis
BC	Boundary Condition
ODE	Ordinary Differential Equation
SDOF	Single Degree of Freedom

CHAPTER ONE : INTRODUCTION

1.1 Background

“Micro-electromechanical systems (MEMS) (Li et al., 2019a)” have become popular in modern technology, previous studies have indicated a significant number of “potential applications such as atomic force microscopes (AFMs), with applications including sensors, biomedical devices, micro-actuators, micro-switches and those energy harvesting devices have taken microbeams as the core element(Li et al., 2019a)”. They have been designed to show high sensitivity to forces, displacements, or environmental changes. Many applications are possible with cantilever microbeams. They can detect very small forces by sensing the deflection or change in resonance frequency during sensing. They are also employed for chemical and biological sensing, where functionalized cantilevers detect specific molecules or biological entities through binding interactions, causing measurable deflections. As actuators, these microbeams convert electrical signals into mechanical movement, which is useful in optical-switch. They are major elements of atomic force microscopy because the deflection of the cantilever creates high-resolution images of the surface at the atomic scale; they are applied in energy harvesting where vibrational energy is converted into electrical energy in micro-devices(Halvorsen & Dong, n.d.). Applied uses in optics include tunable micro-mirrors for light beams to be reflected or modulated with very high precision.

These cantilever microbeams have a high sensitivity that enables them to detect very small forces and displacements and are capable of being scaled down for mass production by standard MEMS processes. Versatility makes them appropriate for sensing, actuation, and energy harvesting applications. They can also be easily integrated into larger MEMS and, more importantly, dovetail with semiconductor technologies currently in use. The main working principles of the cantilever microbeams are based on deflection, where the cantilever flexes upon a force applied to the free end; resonance, in which the natural frequency of a cantilever is changed by a variation of mass or stiffness and thus allows the detection of added masses or environmental changes; piezoresistive/piezoelectric sensing, whereby strain gauges or piezoelectric materials convert the mechanical deformation into easy-to-measure electrical signals.

Circular tapered cantilever microbeams have more advanced mechanical properties than uniform cantilever microbeams and hence are precision devices. However, the geometrical complexity of their shape complicates analytical and numerical modeling. It is the intention of this thesis to investigate vibration characteristics of circular tapered cantilever microbeams using the assume mode technique and a transcendental shape function.

1.2 Problem Statement

In most of the previous studied focused on study of vibrational behavior in uniformly shaped cantilever microbeams. Some researcher has studied tapered cantilever microbeams with rectangular cross section and linear varying geometry. Despite extensive research in microbeams dynamics, there remains a significant gap in understanding the free vibration characteristic of circular tapered cantilever microbeams. The primary objective of this thesis is to determine and validate an analytical solution of circular tapered cantilever microbeams and simulate the model which will accurately predicts the free vibrational response microbeams. The results of this research will not only enhance the design and optimization of MEMS devices but also contribute to the broader field of micro-scale structural dynamics.

1.3 Objectives:

1.3.1 Main Objective:

The main objective of this thesis is free vibrational analysis of circular tapered cantilever microbeams with different tapered ratio.

1.3.2 Specific Objectives:

- To derive the governing differential equation of motion of tapered cantilever microbeams with or without an attached mass at free end, using Lagrange equation and Hamilton Principle.
- To use assume mode method and Transcendental shape function approach to get an analytical solution for tapered cantilever microbeams.
- To determine the effect of various tapered ratio on natural frequency of circular tapered cantilever microbeams.
- To validate the result with Ansys simulation.

1.4 Scope of the Work and Assumptions

This research focused on the free vibration analysis of circular tapered cantilever microbeams with or without an attached mass at free end. In this study assumption were made to developed mathematical model. The analysis is based on different tapered ratio of microbeams. Only first three fundamental bending mode is considered, and beam have constant material properties. The primary objective is to achieve an analytical model for free vibration response. The study centers on the effect of the circular taper on vibration characteristics and verifies the results achieved by comparing with numerical simulations.

Assumptions:

- The microbeams undergoes small displacements.
- The plane cross-sections remain plane and perpendicular to the deformed axis, there is no shear deformation and rotatory inertia effect.
- The microbeams are made of a homogeneous, linear-elastic material.
- The model focuses on free vibration and does not include external damping.

1.5 Organization of the Thesis

This thesis presents an investigation into the Free response of the Cantilever micro beams.

- Chapter 1 outline the fundamental background and objectives of the research.
- extensive literature survey of related past works presents in chapter 2.
- Methodology used to conduct the research is explained in Chapter 3.
- Partial differential equations governing the dynamic behavior of the system are developed in Chapter 4 considering different models.
- Partial differential equations are solved analytically for free response of the system in Chapter 4.
- Simulation and analytical results according the parameter are discussed in chapter 5.
- Conclusions and the scope for recommendation work are discussed in Chapter 6.

CHAPTER TWO : LITERATURE REVIEW

2.1 Overview of a Cantilever Microbeam

Cantilever microbeams is the type of beam with one end fixed and another end free. The study of micro-scale beam Vibration has significant attention in recent times, and it has more demand for microelectromechanical systems (MEMS) and detectors. Early workshop in ray proposition generally grounded on Euler- Bernoulli and Timoshenko phrasings handed a robust foundation for understanding vibrational gets in invariant shafts. These studies generally assumed constant cross-sectional parcels and concentrated on free and forced vibration characteristics under small relegation conditions.

2.1.1 Mathematical Modeling

“When creating a mathematical model, it might be essential to make certain assumptions to eliminate insignificant effects from the analysis and to simplify the problem while maintaining suitable accuracy(Luintel, 2024).

2.1.2 Mathematical Solution

“The governing equation of the motion is subsequently solved utilizing a suitable mathematical approach. An analytical solution in closed form is favored when the governing equation is in a straightforward and standard format (Luintel, 2024).

2.1.3 Assumed Mode Method

“The assumed mode method can be applied alongside the Lagrange equation to transform the governing equations of any continuous system represented by partial differential equations into a set of ordinary differential equations that only have time as the independent variable.(Luintel, 2024)” .

2.1.4 Previous Researches

“The study of the dynamic and vibrations of MEMS (He et al., 2021a, 2021b; Joshi et al., 2019; Pallay & Towfighian, 2017; Parsediya et al., 2015) Controlling vibrations is a crucial challenge in the MEMS sector. Reducing unwanted vibrations is vital for various applications like machinery, pipelines, and aircraft interiors. A considerable effort has been made to find an appropriate solution.

Singh et al., 2016have investigates the mass sensitivity(Gao et al., 2017a) of non-uniform cantilever beams with linear and quartic width variations under both linear and nonlinear responses. Using the nonlinear Euler‑Bernoulli beam equation and Galerkin approximation combined with the method of multiple scales (MMS).

Meesala et al. presented model for cantilever beam with tip mass system, providing a foundation for how an attached mass influence the beam dynamics(Meesala et al., 2018). Joshi et al. developed a distributed MEMS mass sensor that exploits the piezoelectric resonant behaviors of micro cantilevers. Their work highlights the sensitivity of vibration characteristic to mass changes(Joshi et al., 2019).

"Agha Mohammadi et al., 2023have investigated nonlinear dynamics of parametrically excited cantilever beams with a tip mass (Agha Mohammadi et al., 2023; Friswell et al., 2012; Kim et al., 2012; Yaylı et al., 2016)considering nonlinear inertia and duffing-type nonlinearity". Sun et al., 2016Nonlinear vibration analysis of a type of tapered cantilever beams by using an analytical approximate method.

In their work, M. Lajimi et al., 2009 tackled these challenges by developing a simplified finite element model (FEM) to predict the natural frequencies of microbeam with a concentrated end mass. Their study demonstrates that the FEM accurately captures the axial, torsional, and flexural vibrations of the microbeam, with results validated against analytical solutions when the end mass is absent.

The study of micro-scale beam vibration has significant attention in recent times, and it has more demand for micro electromechanical systems (MEMS) and detectors. Early workshop in ray proposition generally grounded on Euler- Bernoulli and Timoshenko (Wong et al., 2019)phrasings handed a robust foundation for understanding vibrational gets in invariant shafts(Schultz et al., 2015).

(Li et al., 2019b)have "investigated Nonlinear dynamics of parametrically excited cantilever beams with a tip mass considering nonlinear inertia and Duffing-type nonlinearity". Nonlinear vibration analysis of a type of tapered "(Attia & Mohamed, 2022; Banerjee et al., 2006; Wang & Li, 2018) cantilever beams by using an analytical approximate method". (Nirmall T & Vimala S, 2013)In their work, tackled these challenges by developing a simplified finite element model (FEM) to free vibration analysis(Ojha & Luintel, n.d.) of circular tapered cantilever micro-beams predict the natural frequencies and mode shapes of a micro-beam with a concentrated end mass.

(M. Lajimi Amir & Amir M. Lajimi, 2009) examines the vibration analysis of non-uniform rod and beam for fundamental understanding of response. expand these studies by analyzing the free vibration of axially tapered microbeam. (Attarnejad et al., 2011) have introduced basic displacement function to improve free vibration analysis accuracy in tapered beam. Where "(M. Abdel-Jaber et al., 2009)has studies the impact of varying section properties with attached mass".

(Bouchaala et al., 2016a, 2016b) have investigated frequency shift in micro and nano cantilever beam resonator for sensing application. In this governing equation of motion for electrostatically cantilever beam with an added point mass were derived. Using "Galerkin method to obtained first-order approximation. (Rahmani et al., 2020)explored the free vibration characteristics of Fictionally graded micro-beam with attached mass. Their findings underscore the need for refined models".

(M. S. Abdel-Jaber et al., 2008) has investigated the natural frequency of elastically restrained tapered beams, providing insight of vibrational behavior. (Akgöz & Civalek, 2013) has extended these studies by analyzing free vibration analysis of axially functionally graded tapered Bernoulli-Euler micro-beam. By using modified couple stress theory.

"(Wang & Li, 2018) investigated the transverse vibration of rotating tapered beams with hollow circular cross-section". Their results highlight that rotational inertia and gyroscopic effect must be carefully accounted. Similarly, Bazoune et al. studied the effect of tapering on natural frequencies in beam. (Banerjee et al., 2006) employed the dynamic stiffness method to conduct a free vibration analysis of tapered beams. Where (Chhantyal et al., 2024)used both polynomial and transcendental mode shape function for free vibration analysis of beams with complex geometries. Their polynomial approach improves convergence by providing a flexible yet accurate representation of the beam's displacement field.

(Gao et al., 2017b) proposed a method to enhance the sensitivity of vibration through used of stepped cantilever micro beam. (He et al., 2021c) Studied the MEMS cantilever beams with variable cross sections and investigated vibration energy for piezoelectric energy harvesting applications.

2.2 Research Gap

Although significant work has been done on the analysis of microbeam vibrations, most research is still focused on uniform or linearly tapered cantilever beams. Dynamic response of circular tapered cantilever microbeams is still not thoroughly researched. In such a structure, the non-linear variation of cross-sectional properties along the beam length introduces complications in the stiffness and mass distribution not well captured by conventional models. The dominant analysis methods have a tendency to linearize or approximate the tapering effect, leading it to potentially fail when determining natural frequencies and mode shapes.

CHAPTER THREE : RESEARCH METHODOLOGY

3.1 Conceptual Framework

The research will be carried out with the following methodology:

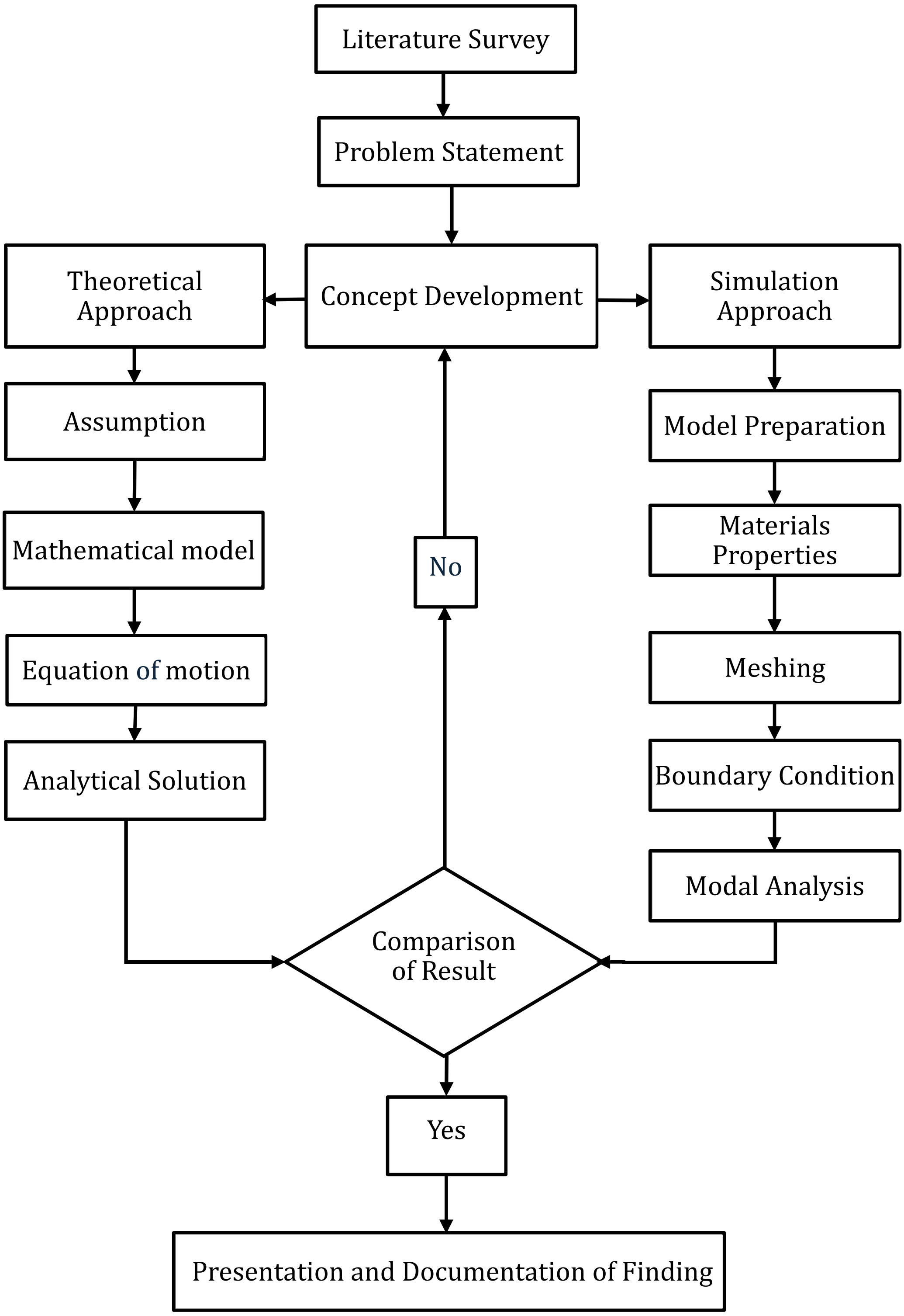

Figure 3.1 Flowchart of research methodology

This chapter describe the methodology of free vibration analysis of circular tapered cantilever microbeam. The research follows a structured approach as shown in figure 3.1 Flowchart of research methodology. The methodology consists of both theoretical and simulation-based analysis to predict the natural frequency.

3.2 Problem Statement

The research focuses on the free vibrational analysis of a circular tapered cantilever micro beam a critical component of MEMS device. Most previous works focus on uniform microbeams, but tapered geometries introduce complexities to be investigated more in depth. Tapered circular cantilever microbeams' responses, especially with the presence of attached mass at the free end.

3.3 Literature Survey

A comprehensive literature review was conducted to get knowledge about vibrational analysis of micro scale beams, the effect of tapered ratio and different beam theory. The internet was utilized to collect previous research in the same Areana. They made use of the IOE's previous thesis and their access to numerous international journals. The relevant prior literature was reviewed and grouped based on the type of issue they addressed, the approach they took, and an extensive evaluation of their main conclusions.

3.4 Concept Development

Based on the literature review and identified research gap the conceptual framework for this study was developed to systematically analyzed the vibration characteristic of circular tapered micro beam.

3.5 Theoretical Approach

mathematical models have Developed based on “Euler-Bernoulli beam theory” for tapered cantilever beams. The differential equations governing the motion were derived and solved using appropriate boundary conditions.

3.5.1 Assumption

- Linearity: The beam experience small deflection, so geometric nonlinearity is negligible.
- The beam consists of silicon materials only.
- In circular tapered the cross-sectional radius varies continuously along the length.

- No damping present.

3.5.2 Mathematical Model

The Euler-Bernoulli beam theory is used to represent the circular tapered cantilever micro beam. The cross-sectional area A(x) and moment of inertia I(x) are defined as functions of axial position x to account tapering.

3.5.3 Equation of motion

Equations of motion for Euler Bernoulli beam model were developed by using assumed mode method and Lagrange's equations into the expressions of kinetic and potential energies of the system

3.5.4 Analytical Solution

The assume mode method and transcendental shape function were used to calculate the modal mass and modal stiffness matrix. The Matlab and Maple software were utilized to calculate natural frequency for first three mode for different tapering ratio.

3.6 Simulation Approach

The Ansys designed modeler were used to developed 3D model of circular micro beam with different tapered ratio. The silicon material properties for the microbeams, including density, Young's modulus, and Poisson's ratio were assigned. The cantilever boundary conditions were applied to the model with 0.2 um mesh refinement.

3.6.1 Modal Analysis

Model analysis was performed to determine the mode shape and natural frequency for first 3 mode.

3.7 Comparison of Results

The results of the theoretical (analytical solutions) and simulation (modal analysis) approaches are compared in a systematic way to validate the method. The most significant parameters, i.e., natural frequencies and mode shapes, are tabulated and graphically plotted to verify agreement. The discrepancies are verified to identify potential causes of error, e.g., oversimplified modeling in the theory (e.g., neglecting shear effects) or insufficient mesh refinement in the simulation. If the results are within tolerable differences (e.g., less than a 15% difference in percentages), the results are considered reliable, and the process proceeds to documentation. If significant differences are found, the method goes back to Concept Development for refinement—revising assumptions, enhancing the mathematical model, or optimizing simulation parameters—and the analysis is repeated until convergence is achieved.

3.8 Report Preparation

The findings of the research work will present in the conferences. Similarly, all findings are compiled as a thesis report as per the requirement of the department of Mechanical and Aerospace engineering and will be submitted to the department.

CHAPTER FOUR : ANALYTICAL AND SIMULATION MODELING

4.1 Problem Formulation Using Euler-Bernoulli Beam Model

4.1.1 System Kinematics

The mathematical model for free vibration analysis of circular tapered cantilever microbeam with attached mass and without attached mass are shown in following figures 4.1 and 4.2.

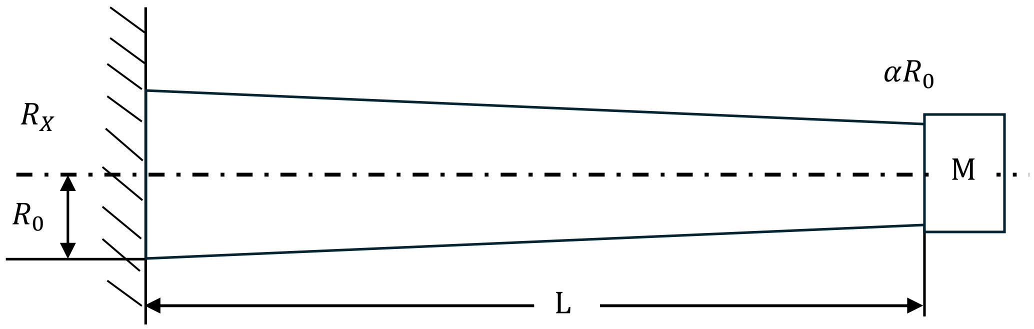

Figure 4.1 Cantilever Micro Beam with attached end mass

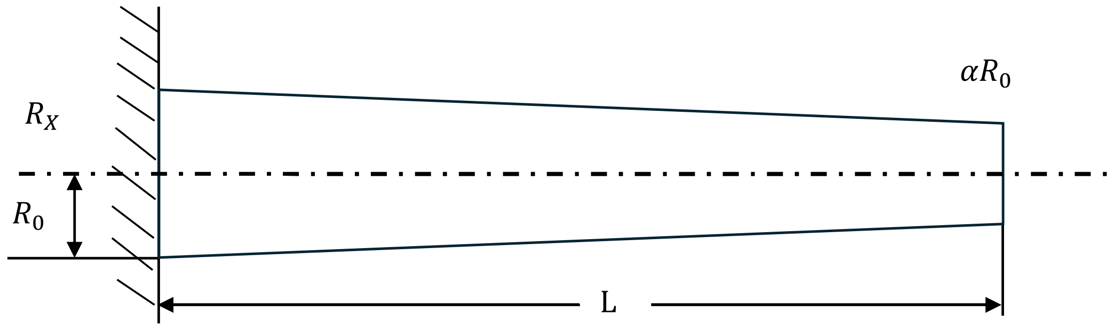

Figure 4.2 Cantilever Micro Beam

Consider a Cantilever microbeam "undergoing transverse deformation due to vibration(Luintel, 2024)". It has Length "L", clamped at x=0 and free at x= L. The beam cross-section is circular and tapered linearly along its length from a radius R (0) = R_0 to, R_0= αL at the free end, where α is the tapering parameter. The micro beam has density "ρ" and modulus of elasticity "E". The beam's transverse deflection is denoted by w (x, t). where x is the coordinate along the beam. M is the attached mass at free end as shown in above figure 4.1. Here radius of circular cross-sectional beam is R(x) and cross–sectional area: $A(x) = \pi R(x)^2$,moment of inertia: $I(x) = \frac{\pi}{4} R(x)^4$

The radius, area, moment of inertia of the circular cantilever micro beam at any position of x are

$$R(x) = R_0[1 + (\alpha - 1)\frac{x}{L}]$$ Eq.(4.1)

$$A(x) = \pi R_0^2[1 + (\alpha - 1)\frac{x}{L}]^2$$ Eq.(4.2)

$$I(x) = \frac{\pi}{4} ER_0^4[1 + (\alpha - 1)\frac{x}{L}]^4$$ Eq.(4.3)

4.2 Energy Expressions for the System

The kinetic energy of the cantilever tapered microbeam is

$$T_b = \frac{1}{2}\int_0^L \pi\rho R_0^2[1 + (\alpha - 1)\frac{x}{L}]^2(\frac{\partial w}{\partial t})^2 dx$$ Eq.(4.4)

The kinetic energy of the mas attached at free end is

$$T_M = \frac{1}{2} M(\frac{\partial w}{\partial t})^2 \,|\, x = L$$ Eq.(4.5)

Thus, the total kinetic energy is

$$T = \frac{1}{2}\int_0^L \pi\rho R_0^2[1 + (\alpha - 1)\frac{x}{L}]^2(\frac{\partial w}{\partial t})^2 dx + \frac{1}{2} M(\frac{\partial w}{\partial t})^2 \,\Big|_{x=L}$$ Eq.(4.6)

The Strain energy of the cantilever tapered microbeam is

$$V = \frac{1}{2}\int_0^L \frac{\pi}{4} ER_0^4[1 + (\alpha - 1)\frac{x}{L}]^4(\frac{\partial^2 w}{\partial x^2})^2 dx$$ Eq.(4.7)

The Lagrangian functional is

$$L = T - v$$ Eq.(4.8)

$$L = \frac{1}{2}\int_0^L \pi\rho R_0^2 \left[1 + (\alpha - 1)\frac{x}{Ll}\right]^2 \left(\frac{\partial w}{\partial t}\right)^2 dx + \frac{1}{2} M \left(\frac{\partial w}{\partial t}\right)^2 \Big|_{x=L} - \frac{1}{2}\int_0^L \frac{\pi}{4} ER_0^4 \left[1 + (\alpha - 1)\frac{x}{L}\right]^4 \left(\frac{\partial^2 w}{\partial x^2}\right)^2 dx$$ Eq.(4.9)

4.3 Derivation of Equation of motion

Now applying Hamilton Principle

$$\delta \int_{t_1}^{t^2} L dt = 0$$ Eq.(4.10)

On solving equation 4.10 then the equation of motion obtained is:

$$\pi\rho R_0^2 \left[1 + (\alpha - 1)\frac{x}{L}\right]^2 \frac{\partial^2 w}{\partial t^2} + M\delta(x - L) + \frac{\pi}{4} ER_0^4 \left[1 + (\alpha - 1)\frac{x}{L}\right]^4 \frac{\partial^2}{dx^2}\left(\frac{\partial^2 w}{\partial x^2}\right) = 0$$ Eq.(4.11)

Associated boundary conditions are:

At fixed end of the beam, where x=0, the transverse displacement w is zero at all times t.

$$w(0,t) = 0 \quad \text{Eq.(4.12)}$$

The slope of the beam's deflection curve at x=0 for all time t.

$$\left(\frac{\partial w}{\partial t}\right)(0,t) = 0 \quad \text{Eq.(4.13)}$$

At X=L has no bending moments

$$EI(L)\left(\frac{\partial w}{\partial t}\right)(L,t) = 0 \quad \text{Eq.(4.14)}$$

At X=L has no shear force.

$$\frac{\partial}{dx}(EI(L)\left(\frac{\partial w}{\partial t}\right))|_{x=L} = 0 \quad \text{Eq.(4.15)}$$

4.4 Assumed Mode Method for Approximate Solution of free response:

"The assumed mode method can be applied alongside Lagrange's equation to transform the governing equation of any continuous system, represented as a partial differential equation, into a set of ordinary differential equations that only contain time as the independent variable, Consider the Lagrangian functional associated with a beam as(Luintel, 2024)" .

$$L = \frac{1}{2}\int_0^L \pi\rho R_0^2 \left[1 + (\alpha - 1)\frac{x}{l}\right]^2 \left(\frac{\partial w}{\partial t}\right)^2 dx + \frac{1}{2}M\left(\frac{\partial w}{\partial t}\right)^2 \Big|_{x=L} - \frac{1}{2}\int_0^L \frac{\pi}{4} E R_0^4 \left[1 + (\alpha - 1)\frac{x}{L}\right]^4 \left(\frac{\partial^2 w}{\partial x^2}\right)^2 dx \quad \text{Eq.(4.16)}$$

Then the approximate solution of w (x, t) can be assumed as

$$w(x,t) = \sum_{i=0}^{n} \emptyset_i(x) q_i(t) \quad \text{Eq.(4.17)}$$

where $\emptyset_i$'s are the functions that are linearly independent and meet the boundary conditions of the problem.

Substituting Eq. 4.17 into Eq. 4.16, we get

$$L = \frac{1}{2}\int_0^L \pi\rho R_0^2 \left[1 + (\alpha - 1)\frac{x}{L}\right]^2 \left(\sum_{i=0}^{n} \emptyset_i(x)\dot{q}_i(t)\right)^2 dx + \frac{1}{2}M\left(\sum_{i=0}^{n} \emptyset_i(x)\dot{q}_i(t)\right)^2 |_{x=L} dx - \int_0^L \frac{\boldsymbol{\pi}}{\mathbf{4}} \mathbf{E}\mathbf{R}_\mathbf{0}^\mathbf{4} \left[\mathbf{1} + (\boldsymbol{\alpha} - \mathbf{1})\frac{\mathbf{x}}{\mathbf{L}}\right]^\mathbf{4} \left(\sum_{i=0}^{n} \emptyset''_i(x) q_i(t)\right)^\mathbf{2} dx$$

$$+\frac{1}{2}M\left(\sum_{i=0}^{n}\emptyset_i(x)\dot{q}_i(t)\right)^2 \mid dx_{x=L}$$

Now applying Lagrange equation for a general coordinate q_i, we get

$$\int_0^L \pi\rho R_0^2 \left[1+(\alpha-1)\frac{x}{L}\right]^2 \emptyset_i(x)\left(\sum_{i=0}^{n}\emptyset_i(x)\ddot{q}_t(t)\right)dx$$

$$+\frac{1}{2}M\emptyset_i(x)\left(\sum_{i=0}^{n}\emptyset_i(x)\ddot{q}_t(t)\right)\Big|_{x=L} dx$$

$$-\int_0^L \frac{\pi}{4}ER_0^4\left[1+(\alpha-1)\frac{x}{L}\right]^4 \emptyset''_i(x)\left(\sum_{i=0}^{n}\emptyset''_i(x)q_i(t)\right)^2 dx = 0$$

Combining such equations for all general coordinates' qi 's in matrix form, we get

$$[M]\{\ddot{q}_t\} + [k]\{q_i(t)\} = 0 \qquad \text{Eq.(4.18)}$$

where the elements of matrices [K] and [M] are given respectively as

$$K_i = \int_0^L \frac{\pi}{4}ER_0^4\left[1+(\alpha-1)\frac{x}{L}\right]^4 \emptyset^{iv}{}_i(x)\emptyset_i(x)dx \qquad \text{Eq.(4.19)}$$

$$M_i = \int_0^L \pi\rho R_0^2 \left[1+(\alpha-1)\frac{x}{L}\right]^2 \emptyset_i^2(x)\,dx + M\emptyset_i^2(L) \qquad \text{Eq.(4.20)}$$

4.5 Frequency from Mathematical Model

With values of modal stiffness and modal mass obtained from equation 4.19 and 4.20 the natural frequency of tapered circular microbeams obtained as

$$\text{Natural frequency } w_n = \sqrt{\left(\frac{K_i}{M_i}\right)} \qquad \text{Eq.(4.21)}$$

4.6 Transcendental Mode Shape Function

The following transcendental mode shape function is used to get the modal mass modal stiffness (Chhantyal et al., 2024; Luintel, 2021; Rao, 2011).

$$\emptyset_i = c_i[\cosh(\beta_i x) - \cos(\beta_i x) - \frac{\cosh(\beta_i L)+\cos(\beta_i L)}{\sinh(\beta_i L)+\sin(\beta_i L)}(\sinh(\beta_i x) - \sin(\beta_i x))] \qquad \text{Eq.(4.22)}$$

c_i is a constant for normalized mode shape, $\beta_i$is the wave number, x is the position along the beam. The eigen values are determined from the frequency equation.

$$\cos\beta_i\cosh\beta_i l + 1 = 0 \qquad \text{Eq.(4.23)}$$

Where the eigen values for cantilever micro beam are

$$\beta_1 L = 1.875104 \qquad \text{Eq.(4.24)}$$

$$\beta_2 L = 4.694091 \qquad \text{Eq.(4.25)}$$

$$\beta_3 L = 7.854757 \qquad \text{Eq.(4.26)}$$

The Transcendental Mode Shape Function for first mode is

$$\emptyset_1 = c_1[\cosh(1.875104x) - \cos(1.875104\beta_i x) - \frac{\cosh(1.875104L) + \cos(1.875104L)}{\sinh(1.875104L) + \sin(1.875104L)}(\sinh(1.875104x) - \sin(1.875104x))] \qquad \text{Eq.(4.27)}$$

Where c_1 found that 1

The normalized mode shape for first mode is then

$$\emptyset_1 = [\cosh(1.875104x) - \cos(1.875104\beta_i x) - \frac{\cosh(1.875104L) + \cos(1.875104L)}{\sinh(1.875104L) + \sin(1.875104L)}(\sinh(1.875104x) - \sin(1.875104x))] \qquad \text{Eq.(4.28)}$$

The Transcendental Mode Shape Function for second mode is

$$\emptyset_2 = c_2[\cosh(4.694091x) - \cos(4.694091\beta_i x) - \frac{\cosh(4.694091L) + \cos(4.694091L)}{\sinh(4.694091L) + \sin(4.694091L)}(\sinh(4.694091x) - \sin(4.694091x))] \qquad \text{Eq.(4.29)}$$

Where c_2 found that 0.56

The normalized mode shape for first mode is then

$$\emptyset_2 = \frac{1}{0.56}[\cosh(4.694091x) - \cos(4.694091\beta_i x) - \frac{\cosh(4.694091L) + \cos(4.694091L)}{\sinh(4.694091L) + \sin(4.694091L)}(\sinh(4.694091x) - \sin(4.694091x))] \qquad \text{Eq.(4.30)}$$

The Transcendental Mode Shape Function for Third mode is

$$\emptyset_3 = c_3[\cosh(7.854757x) - \cos(7.854757x) - \frac{\cosh(7.854757L) + \cos(7.854757L)}{\sinh(7.854757L) + \sin(7.854757L)}(\sinh(7.854757x) - \sin(7.854757x))] \qquad \text{Eq.(4.31)}$$

Where c_2 found that 0.38

Then the normalized mode shape is

$$\emptyset_3 = \frac{1}{0.38}\left[\cosh(7.854757x) - \cos(7.854757x) - \frac{\cosh(7.854757L) + \cos(7.854757L)}{\sinh(7.854757L) + \sin(7.854757L)}(\sinh(7.854757x) - \sin(7.854757x))\right] \quad \text{Eq.(4.32)}$$

4.7 Simulation Model

The 3D circular tapered cantilever micro-beam as shown in figure 4.3 with different tapered ratio with or without attached mass both condition micro-beam is modeled based on theoretical model. Which were developed in Ansys Design modeler.

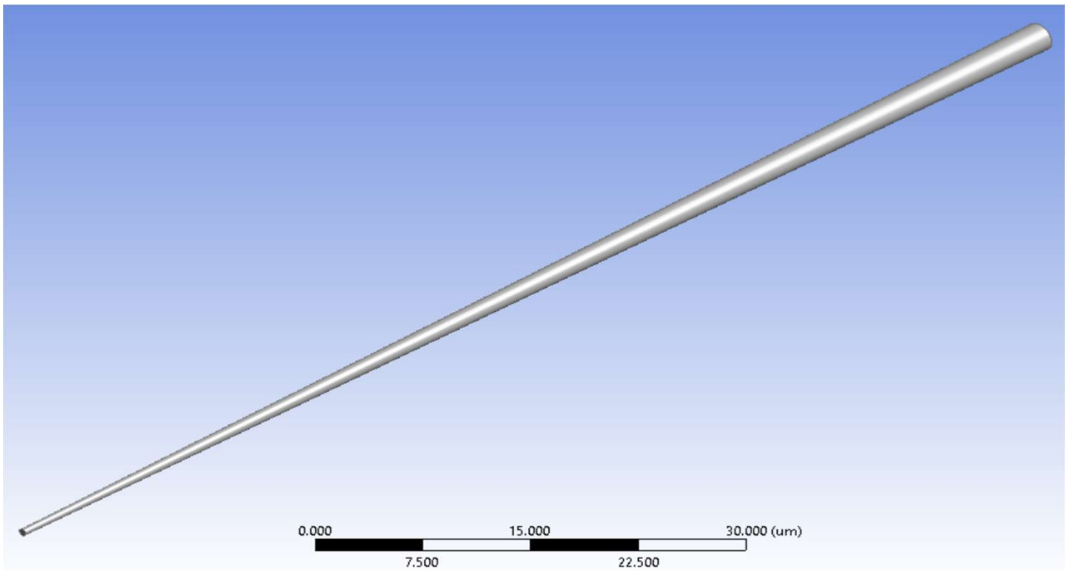

Figure 4.3 3D Model of Circular Tapered Cantilever Beam

4.7.1 Mesh Generation

The details of mesh generation for simulation analysis are shown in following figure 4.4.

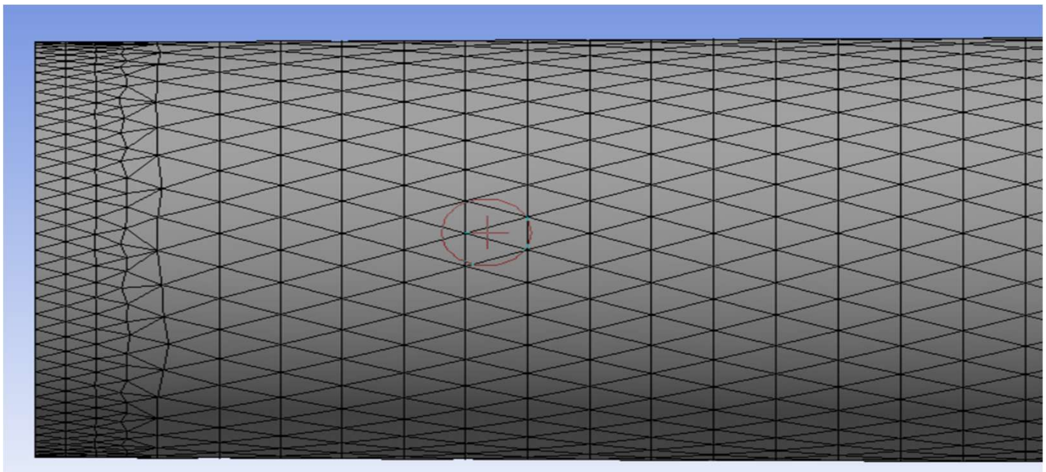

Figure 4.4Mesh Generation of Section of Circular Tapered Cantilever Beam

“A pre-processing step for the computational field simulation is the discretization of the domain of interest and is called mesh generation(Sadrehaghighi, n.d.),(Maharjan & Luintel, 2025)”. The Finite Element tetrahedral mesh in Figure 3 discretized a tapered cantilever microbeam for modal analysis. It consists of 199,561 nodes and 120,443 tetrahedral elements with an element size of 2×10^{-7} m, ensuring Hight resolution for accurate vibrational analysis. The mesh refinement was performed at both end edges. The details of mesh generation are shown in figure 4.4.

4.7.2 Boundary Condition

For Ansys simulation the details of applied boundary condition for both the case with or without an attached mass of cantilever microbeam shown in following figure 4.5.

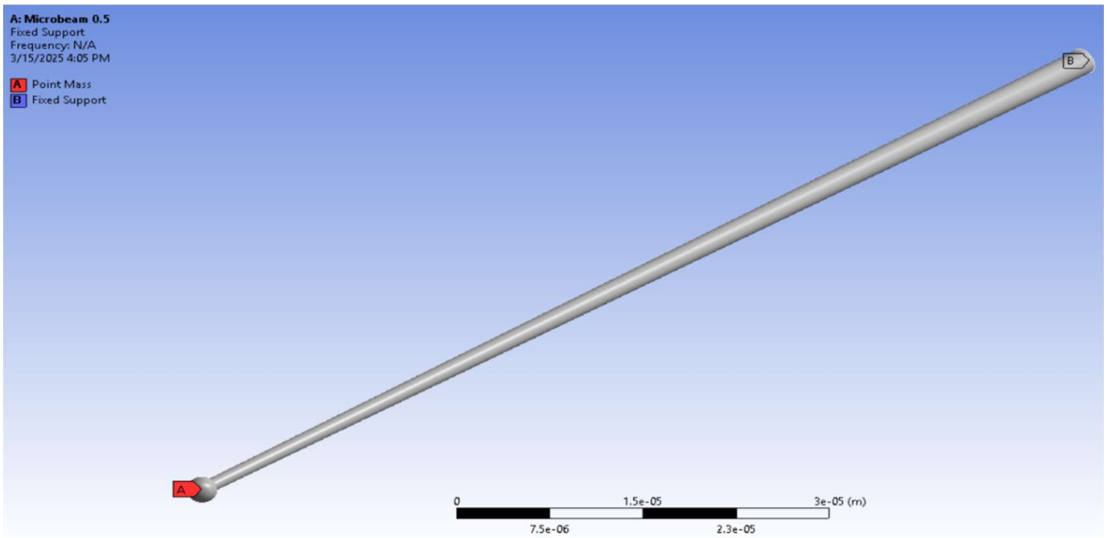

Figure 4.5 Boundary condition applied to Circular Tapered

The details of boundary condition applied in model analysis shown in above Figure 4.5 Cantilever Beam In this modal analysis, the circular tapered cantilever micro-beam is fixed at point B to enforce zero displacement and rotation. A point mass $M = 0.4\times 10^{-12}$ kg is attached at the free end. These boundary conditions align with the theoretical governing equation, and transcendental mode shapes are accurately captured in the FEA analysis. The length, 100 µm, and tapering ($R0 = 1.22$ µm, $\alpha = 0.5 - 1.5$) are evaluated to compute the natural frequency and validate the analytical results.

CHAPTER FIVE : RESULTS AND DISCUSSION

5.1 System parameter

To compare Simulation based result with the classical analytical results. The Material and parameter are taken as in the table 5.1.

Table 5.1 Parameters of the circular Tapered Cantilever Microbeam.

S. N	Parameter	Symbol	Values
1	Length	L	100 µm
2	Radius at Fixed End	R_0	1.22 µm
3	Density	ρ	2330 kg/m³
4	Young's Modulus	E	160 GPa
5	Tapering Parameter	α	0.5,1,1.5
6	Poisson's Ratio	ν	0.28
7	attached at tip Mass	M	0.4×10^{-12} kg
8	Cross-sectional Area at fixed End	A(x)	4.676×10^{-12} m²
9	Moment of inertia at fixed End	I(x)	1.740×10^{-24} m⁴

The table 5.1 summarized the key geometric and material parameters used to for numerical calculation and Ansys simulation. The length of the microbeams is set to 100 µm, and radius at fixed end R_0 is taken as 1.22 µm. The microbeams composed of silicon materials for MEMS application. The density young's modulus of elasticity, poison's ratio was taken for silicon. 0.4×10^{-12} kg tip mass attached at free end of cantilever microbeam.

5.2 Modal Analysis of Circular Tapered Cantilever Micro-Beam without attached mass

In this study at first the analysis was performed without addition of mass at free end of circular tapered cantilever micro-beam. The simulation result was then compared with result from analytical method. The comparison of natural frequencies for the first three modes of vibration for different tapered ratio is presented in Table 5.2,5.3,5.4.

5.2.1 Comparison of Natural Frequencies (MHz) from Simulation and Analytical Methods For $\alpha = 0.5$

The first three bending mode shape of circular tapered cantilever microbeam without attached mass are shown in figure 5.1, 5.2 and 5.3. Each curve shown the shape of n^{th} vibrational mode along the beam normalized length.

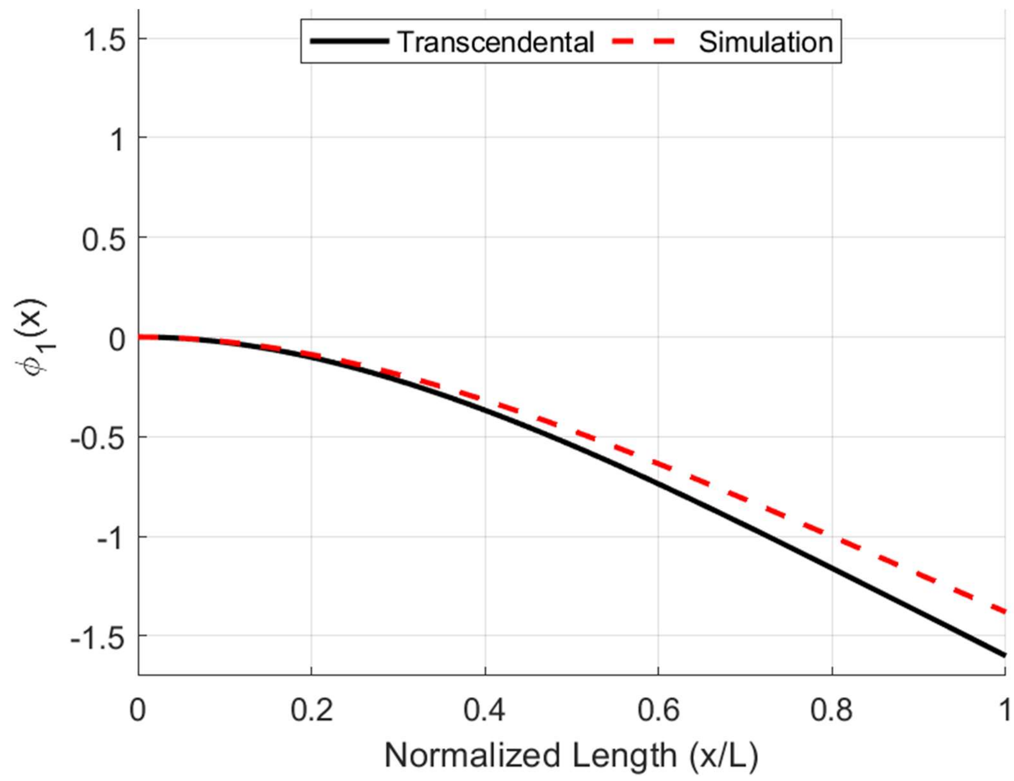

Figure 5.1 First mode shapes Analytical Method and Simulation

The figure (5.1) is the fundamental bending mode. There is no internal node in the interior of the beam. The deflection is large at free end and zero at fixed end.

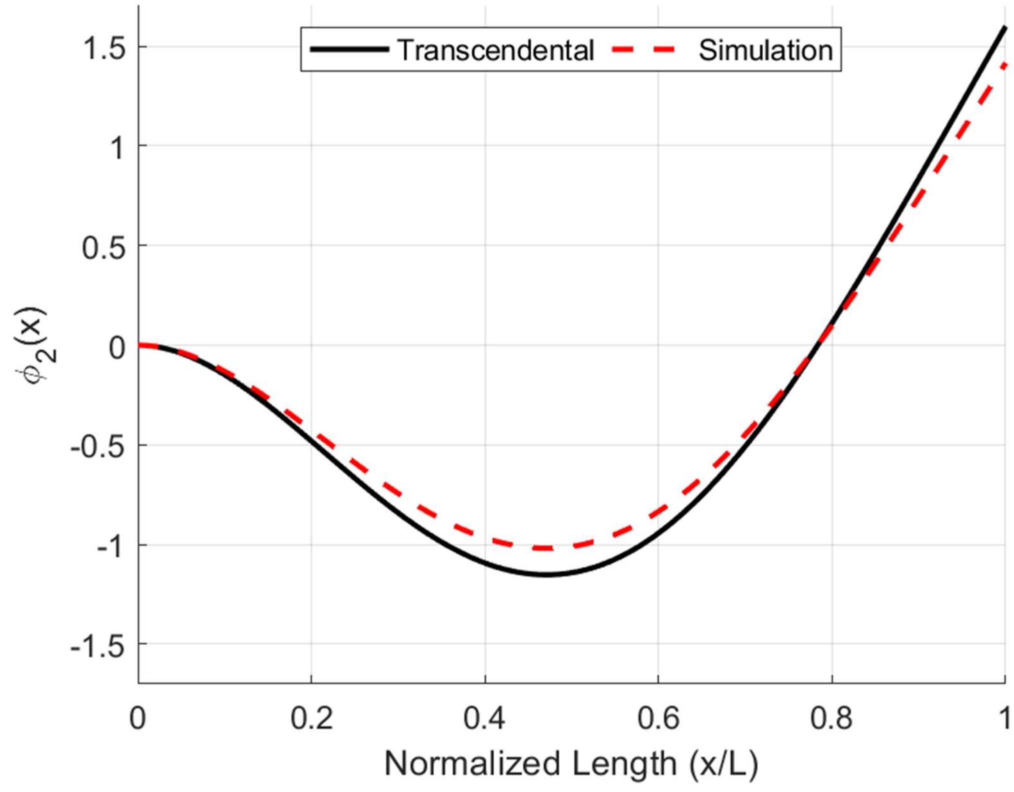

Figure 5.2 Second mode shapes Analytical Method and Simulation

The figure (5.2) is the second bending mode which have one internal node in the interior of the beam. The defection is crossing the zero once with the domain.

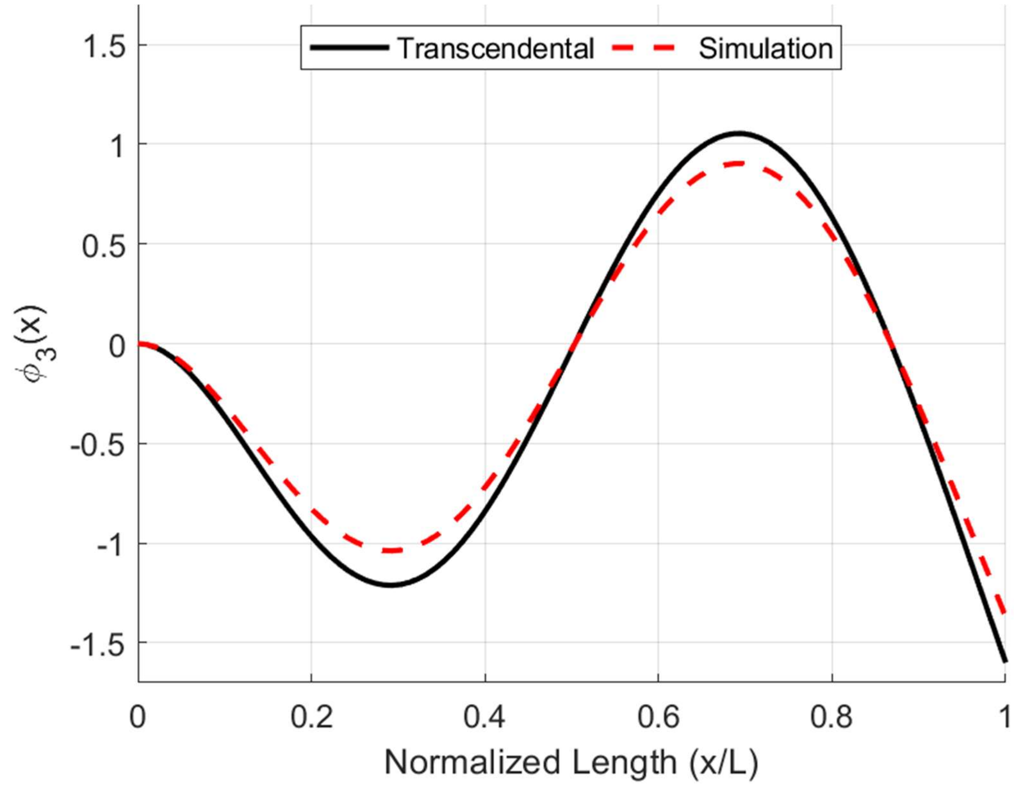

Figure 5.3 Third mode shapes Analytical Method and Simulation

The figure 5.3 is the third bending mode which have two internal nodes in the interior of the beam. The defection is crossing the zero deflection twice its length.

The total deformation of the beam corresponding to first, Second, third modes for alpha $\alpha = 0.5$ are shown in figure 5.4,5.5,5.6.

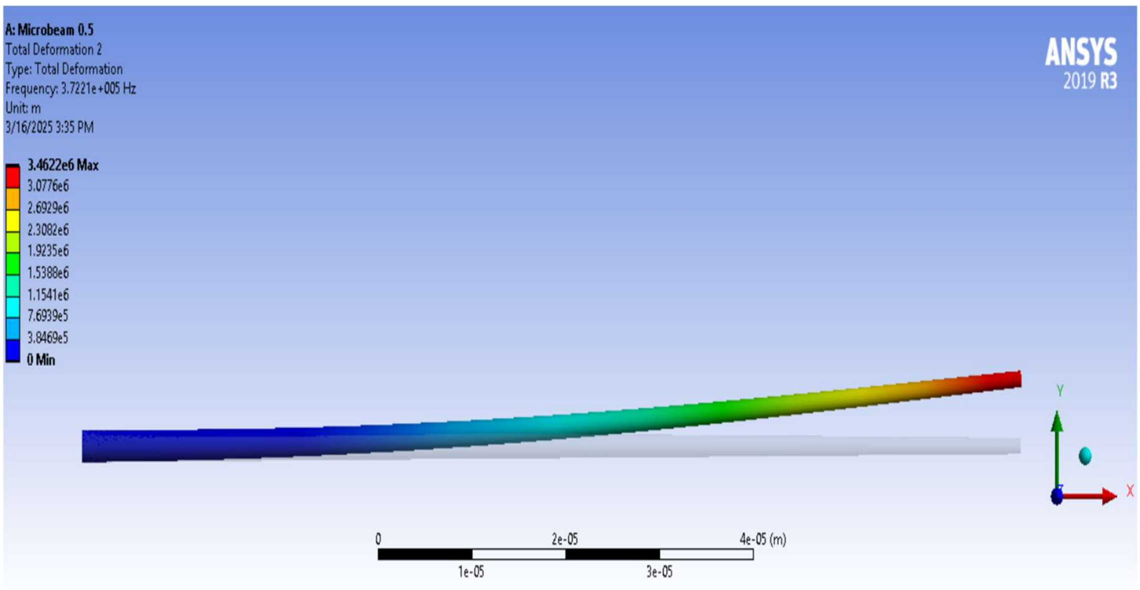

Figure 5.4 Total deformation of the beam corresponding to first mode

Figure 5.4 present the finite element analysis of circular microbeam's vibrational mode shape for first bending mode obtained using Ansys. A color scale indicates the distribution of total deformation along the beam's length. In this mode shape blue color represent lowest deformation and red indicate the highest deformation. From the figure 5.4 the maximum deformation occurs at free end. In the first mode the maximum frequency and deformation obtained as 0.372 MHZ 3.46 µm, deformation decreases linearly from fixed end for first bending mode.

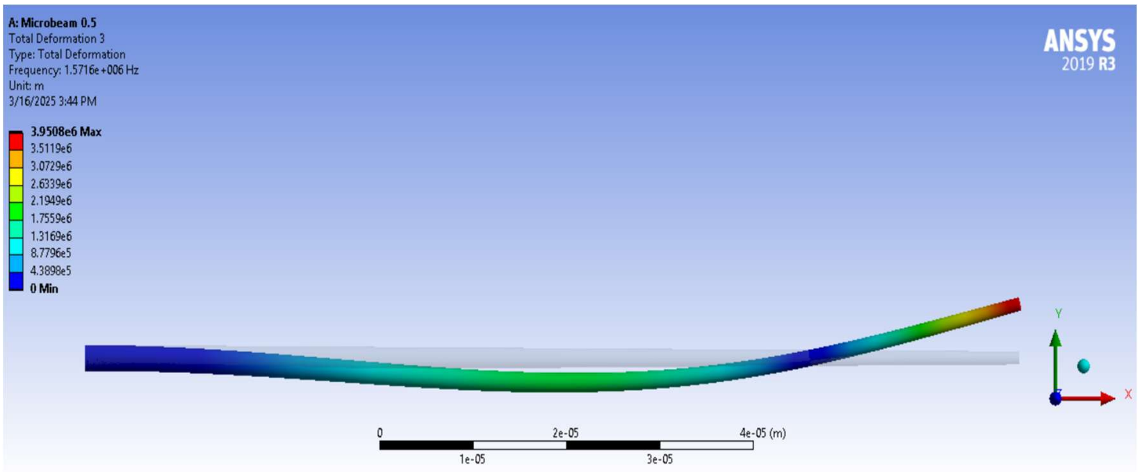

Figure 5.5 Total deformation of the beam corresponding to second mode

Figure 5.5 present the finite element analysis of circular microbeam's vibrational mode shape for first bending mode obtained using Ansys. A color scale indicates the distribution of total deformation along the beam's length. In this mode shape blue color represent lowest deformation and red indicate the highest deformation. From the figure 5.5 the maximum deformation occurs at mid-span of the beam. In the Second mode the maximum frequency and deformation obtained as 1.57 MHZ 3.95 µm.

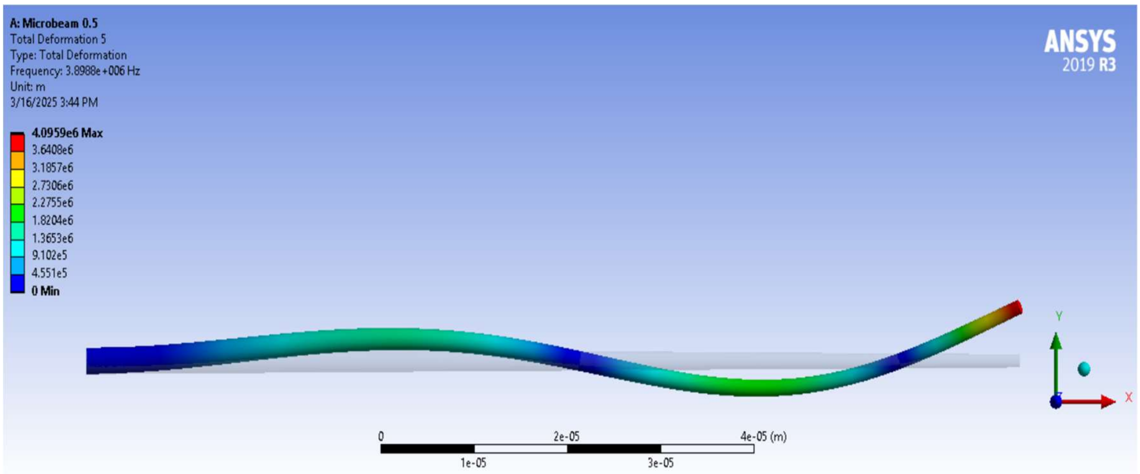

Figure 5.6 Total deformation of the beam corresponding to third mode

Figure 5.6 present the finite element analysis of circular microbeam's vibrational mode shape for third bending mode without attached mass obtained using Ansys. A color scale indicates the distribution of total deformation along the beam's length. In this mode shape blue color represent lowest deformation and red indicate the highest deformation. From the figure 5.6 the minimum equals to zero deformation occurs at midspan. In the third bending mode the maximum frequency and deformation obtained as 3.89 MHZ 4.09 μm.

The details comparison of simulation and analytical results are shown in below table 5.2.

Table 5.2 Natural Frequencies from Simulation and Analytical Methods for first three mode for α=0.5 without attached mass

Mode	Simulation (MHZ)	Analytical (MHZ)	Deviation
1	0.37068	0.3914817	5.31%
2	1.56520	1.6926545	7.53%
3	3.88300	4.2807584	9.29%

Table 5.2 compares the natural frequencies of the first three bending modes of circular tapered cantilever microbeam for α = 0.5, as obtained from numerical simulation and analytical solution. For the first mode, the simulation result is 0.37068 MHz, while the analytical solution is 0.3914817 MHz, resulting 5.31% deviation. Similarly for second mode and third mode the deviation found to be 7.53% and 9.29% respectively. These results demonstrate good agreement between the simulation and the analytical approach, with all deviations under 10%.

5.2.2 Comparison of Natural Frequencies (MHz) from Simulation and Analytical Methods For $\alpha = 1$

The comparison of natural frequency (MHz) for first three fundamental bending modes for α = 1 without attached end mass are shown in table 5.3.

Table 5.3 Natural frequencies from simulation and analytical methods for the first three modes for (α = 1) without an attached mass

Mode	Simulation (MHZ)	Analytical (MHZ)	Deviation
1	0.28300	0.2828673	0.05%
2	1.77000	1.7726991	0.15%
3	4.94000	4.9636089	0.48%

Table 5.3 compares the natural frequencies of the first three bending modes of circular tapered cantilever microbeam for α = 1 as called uniform cantilever micro beam used in this research, as result obtained from numerical simulation and

analytical solution. For the first mode, the simulation result is 0.28300MHz, while the analytical solution is 0.2828673 MHz, resulting 0.05% deviation. Similarly for second mode and third mode the deviation found to be 0.15% and 0.48% respectively. These results demonstrate good agreement between the simulation and the analytical approach, with all deviations under 0.5%.

5.2.3 Comparison of Natural Frequencies (MHz) from Simulation and Analytical Methods For α = 1.5`

The comparison of natural frequency (MHz) for first three fundamental bending modes for α = 1.5 without attached end mass are shown in table 5.4.

Table 5.4 Natural Frequencies from Simulation and Analytical Methods for first three mode for α = 1.5 without attached mass

Mode	Simulation (MHZ)	Analytical (MHZ)	Deviation
1	0.23771	0.2458810	3.32%
2	1.95080	2.0284180	3.83%
3	5.88440	6.1474424	4.28%

Table 5.4 compares the natural frequencies of the first three bending modes of circular tapered cantilever microbeam for α = 1.5 as result obtained from numerical simulation and analytical solution. For the first mode, the simulation result is 0.23771 MHz, while the analytical solution is 0.2458810 MHz, resulting 3.32% deviation. Similarly for second mode and third mode the deviation found to be 3.83% and 4.28% respectively. These results demonstrate good agreement between the simulation and the analytical approach, with all deviations under 4.2%.

5.3 Modal Analysis of Circular Tapered Cantilever Microbeams with Attached Mass

In this study the analysis was performed with addition of point mass at free end of circular tapered cantilever micro-beam. The simulation result was then compared with result from Analytical Method. The Comparison of Natural Frequencies for the first three modes of vibration for different tapered ratio is presented in Table 5.5,5.6,5.7.

5.3.1 Comparison of Natural Frequencies (MHz) from Simulation and Analytical Methods For α = 0.5

The first three bending mode shape of circular tapered cantilever microbeam with attached mass are shown in figure 6.7, 6.8 and 6.9. Each curve shown the shape of nth vibrational mode along the beam normalized length.

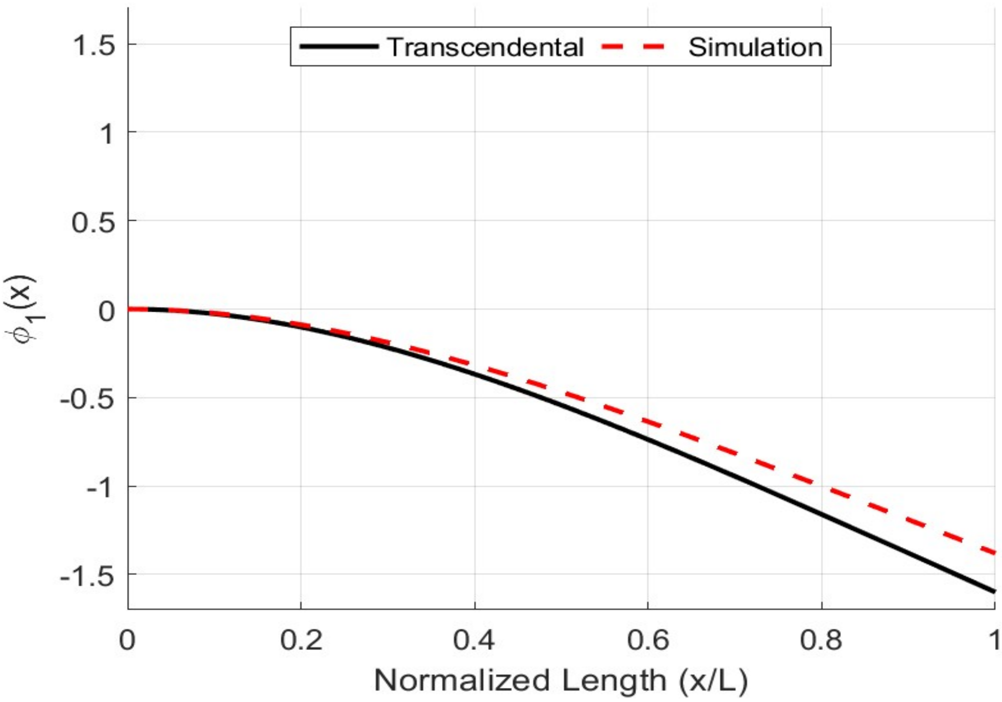

Figure 5.7 First mode shapes Analytical Method and Simulation

The figure 5.7 is the fundamental bending mode. There is no internal node in the interior of the beam. The defection is large at free end and zero at fixed end.

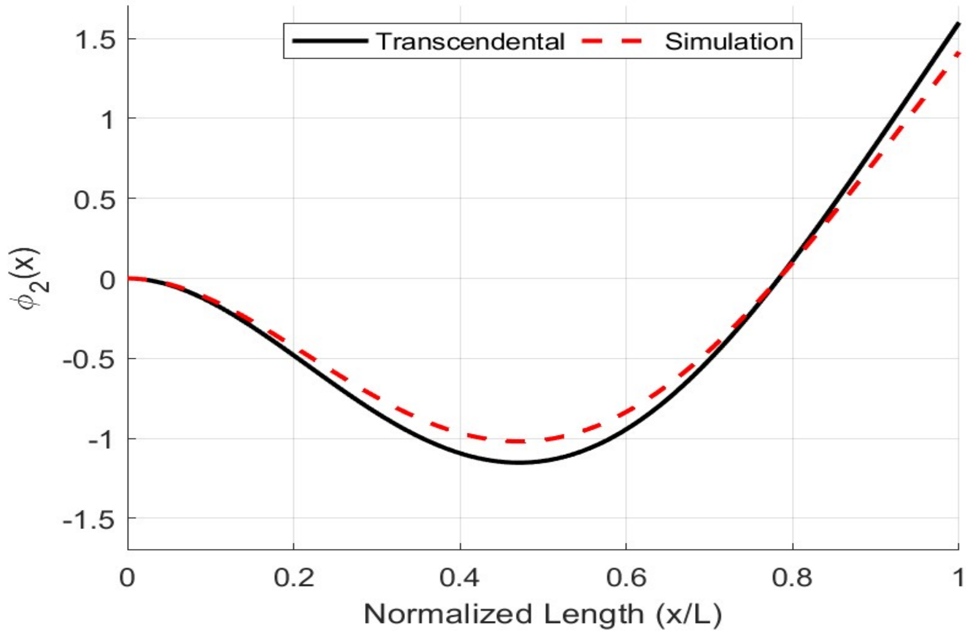

Figure 5.8 Second mode shapes Analytical Method and Simulation

The figure 5.8 is the second bending mode which have one internal node in the interior of the beam. The defection is crossing the zero once with the domain.

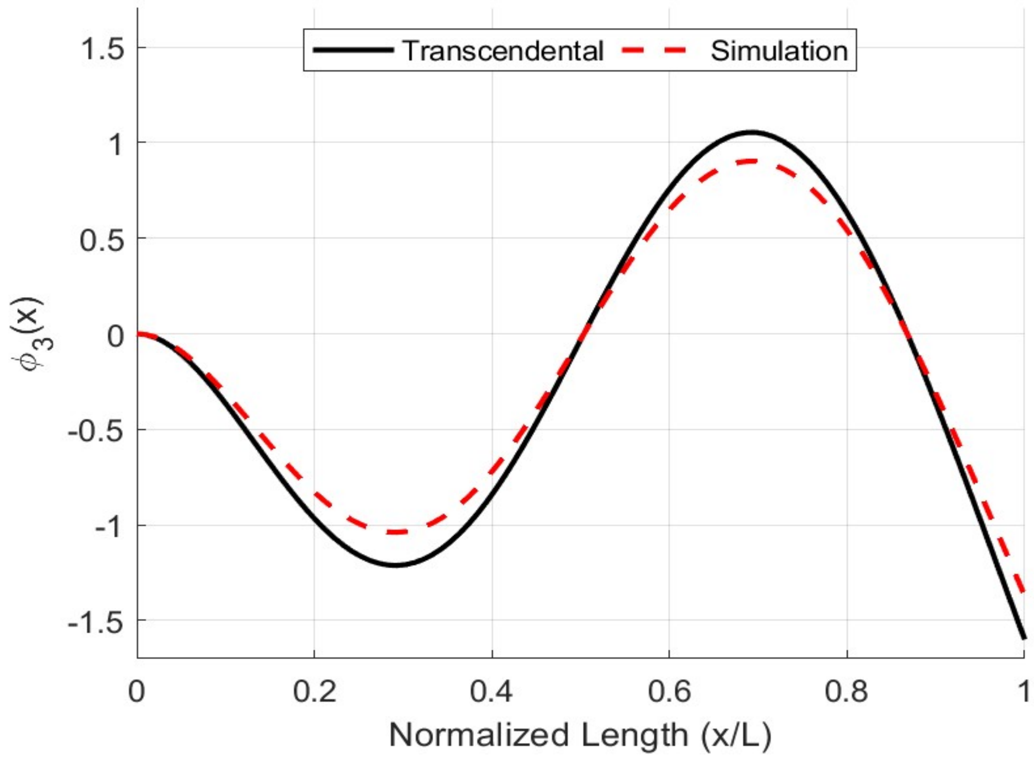

Figure 5.9 Third mode shapes Analytical Method and Simulation

The figure 5.9 is the third bending mode which have two internal nodes in the interior of the beam. The defection is crossing the zero deflection twice its length. The total deformation of the micro beam with attached mass corresponding to first, Second, third modes for alpha α = 0.5 are shown in figure 6.10, 6.11, 6.12.

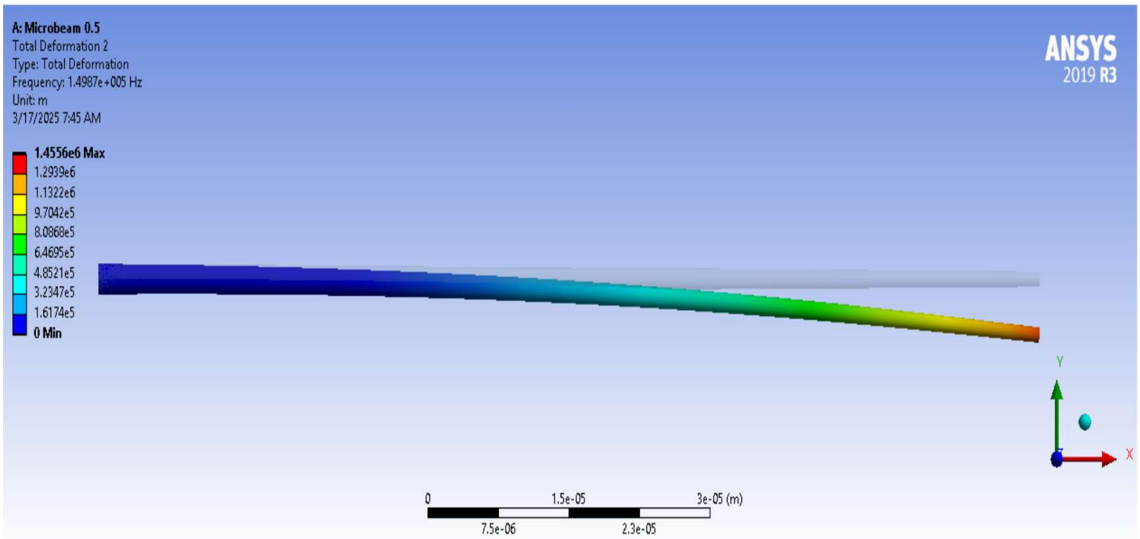

Figure 5.10 Total deformation of the beam corresponding to first mode for alpha 0.5

Figure 5.10 present the finite element analysis of circular microbeam's vibrational mode shape for first bending mode with an attached end mass obtained using Ansys.

A color scale indicates the distribution of total deformation along the beam's length. In this mode shape blue color represent lowest deformation and red indicate the highest deformation. From the figure 5.10 the maximum deformation occurs at free end. In this mode the maximum frequency and deformation obtained as 0.1498 MHZ 1.45 µm. Deformation decreases linearly from fixed end for first bending mode. The frequency decreased due to attached mass.

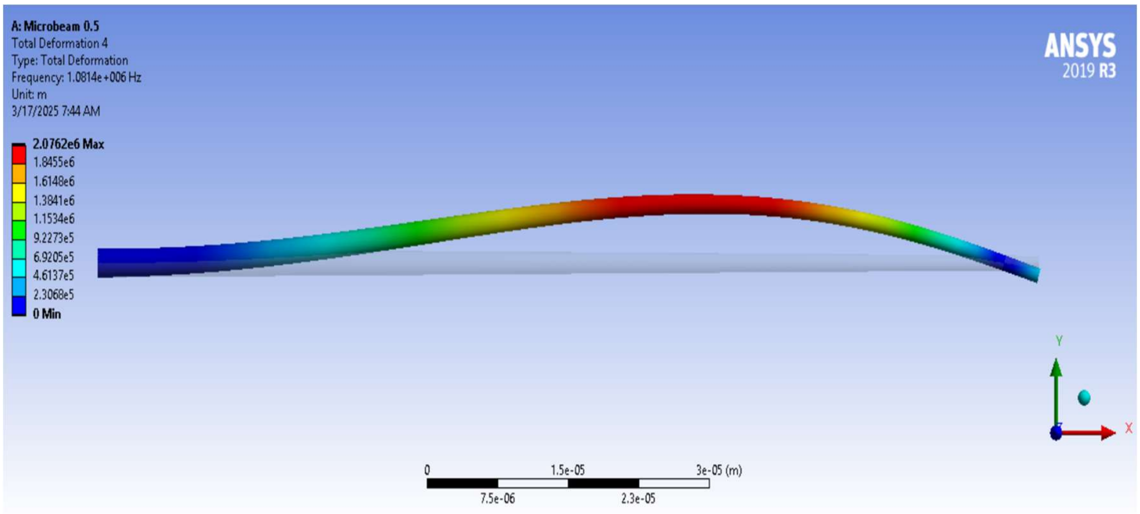

Figure 5.11 Total deformation of the beam corresponding to Second mode

Figure 5.5 present the finite element analysis of circular microbeam's vibrational mode shape for second bending mode with attached obtained using Ansys. A color scale indicates the distribution of total deformation along the beam's length. In this mode shape blue color represent lowest deformation and red indicate the highest deformation. From the figure 5.5 the maximum deformation occurs at mid span of the beam. In the second bending mode the maximum frequency and deformation obtained as 1.081 MHZ 2.05µm.

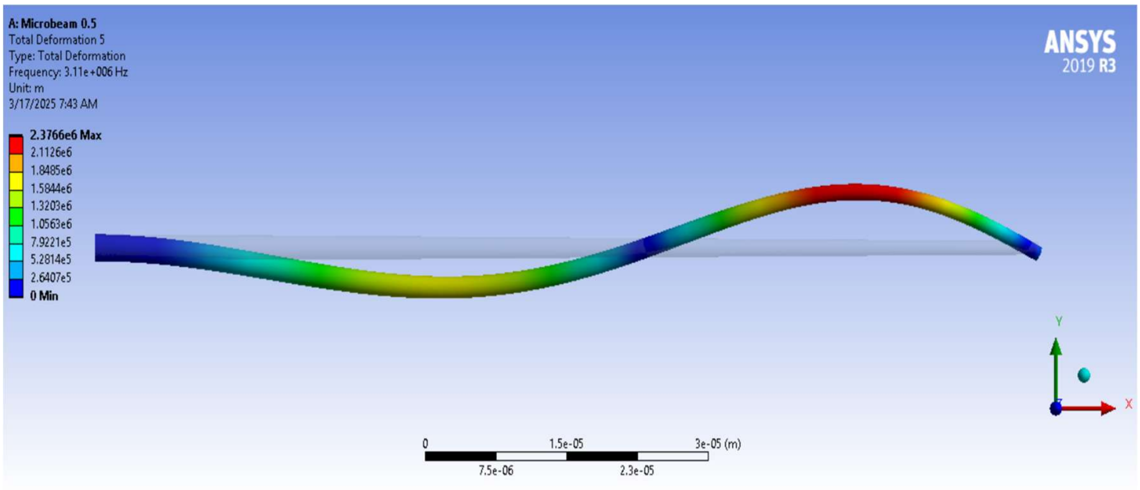

Figure 5.12 Total deformation of the beam corresponding to Third mode

Figure 5.12 present the finite element analysis of circular microbeam's vibrational mode shape for third bending mode with attached mass obtained using Ansys. A color scale indicates the distribution of total deformation along the beam's length. In this mode shape blue color represent lowest deformation and red indicate the highest deformation. From the figure 5.12 the minimum equals to zero deformation occurs at midspan. In the third bending mode with attached mass the maximum frequency and deformation obtained as 3.11 MHZ 2.37μm.

For α = 0.5 in both simulation and analytical methods, the natural frequency increases as the mode number increases. The maximum deviation was found to be less than 14.3%. For α = 0.5 in both simulation and analytical.

Table 5.5Natural Frequencies from Simulation and Analytical Methods for first three mode for α = 0.5 with an attached mass

Mode	Simulation (MHZ)	Analytical (MHZ)	Deviation
1	0.14987	0.1737023	13.72%
2	1.08140	1.2223060	11.53%
3	3.11010	3.6292369	14.30%

Table 5.5 compares the natural frequencies of the first three bending modes of circular tapered cantilever microbeam for α = 0.5 with attached end mass as result obtained from numerical simulation and analytical solution. For the first mode, the simulation result is 0.14987 MHz, while the analytical solution is 0.1737023MHz, resulting 13.72% deviation. Similarly for second mode and third mode the deviation found to be 11.53% and 14.30% respectively. These results demonstrate good agreement between the simulation and the analytical approach, with all deviations under 14.3%.

5.3.2 Comparison of Natural Frequencies (MHz) from Simulation and Analytical Methods For α = 1

The table 6 shows the Comparison of Natural Frequencies (MHz) from Simulation and Analytical Methods For α = 1 with attached mass.

Table 5.6 Natural Frequencies from Simulation and Analytical Methods for first three mode for α = 1

Mode	Simulation (MHZ)	Analytical (MHZ)	Deviation
1	0.19916	0.179743	0.3%
2	1.38970	1.464430	5.1%
3	4.18510	4.501117	7.0%

Table 5.6 compares the natural frequencies of the first three bending modes of circular tapered cantilever microbeam for α = 1 with attached end mass as called uniform cantilever micro beam used in this research, as result obtained from numerical simulation and analytical solution. For the first mode, the simulation result is 0.19916 MHz, while the analytical solution is 0.179743 MHz, resulting 0.3% deviation. Similarly for second mode and third mode the deviation found to be 5.1% and 7% respectively. These results demonstrate good agreement between the simulation and the analytical approach, with all deviations under 7%.

5.3.3 Comparison of Natural Frequencies (MHz) from Simulation and Analytical Methods For α = 1.5

The table 5.7 shows the Comparison of Natural Frequencies (MHz) from Simulation and Analytical Methods For α = 1.5.

Table 5.7 Natural Frequencies from Simulation and Analytical Methods for first three mode for α= 1.5 with attached mass

Mode	Simulation (MHZ)	Analytical (MHZ)	Deviation
1	0.18205	0.1860110	2.13%
2	1.66180	1.7976861	7.56%
3	5.21750	5.7772910	9.69%

Table 5.7 compares the natural frequencies of the first three bending modes of circular tapered cantilever microbeam for α = 1.5 with attached end mass, as result obtained from numerical simulation and analytical solution. For the first mode, the simulation result is 0.18205 MHz, while the analytical solution is 0.186011 MHz, resulting 2.13% deviation. Similarly for second mode and third mode the deviation found to be 7.56% and 9.69% respectively. These results demonstrate good agreement between the simulation and the analytical approach, with all deviations under 10%.

5.4 Frequency Shift due to attached mass

The frequency shift due to attached mass for both cases with or without attached mass are shown in following figures 5.13 and 5.14. In this analysis the attached mass is 62.29% of the beam's, mass for α=05 and 36.7% for α=1. Due to higher mass ratio the frequency shift is more and frequency drop rate decreased with increase in tapered ratio.

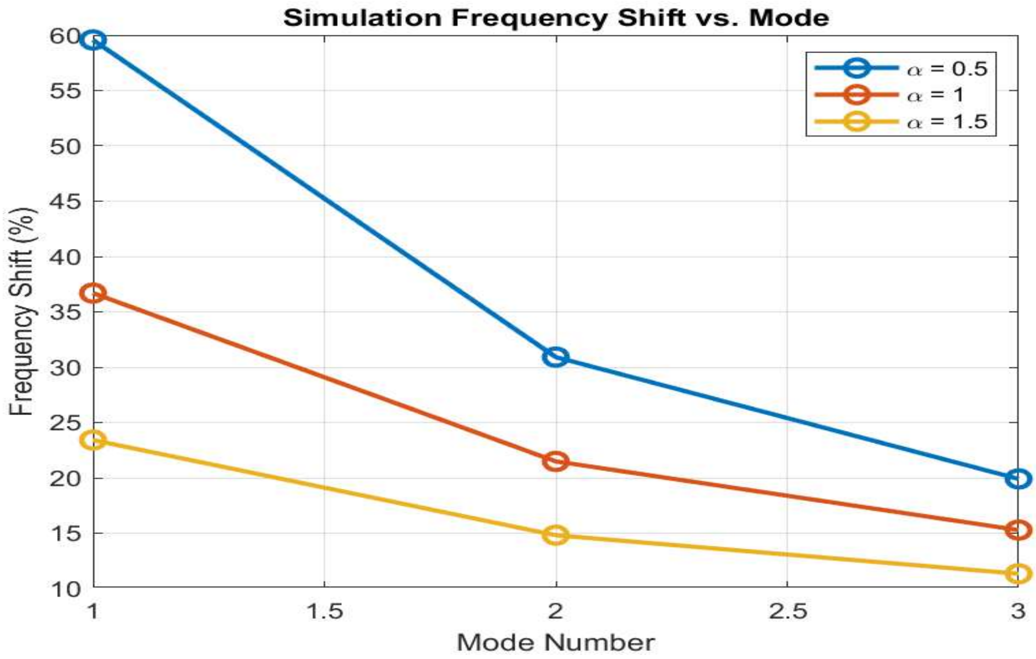

Figure 5.13 Frequency Shift due to add mass in simulation model

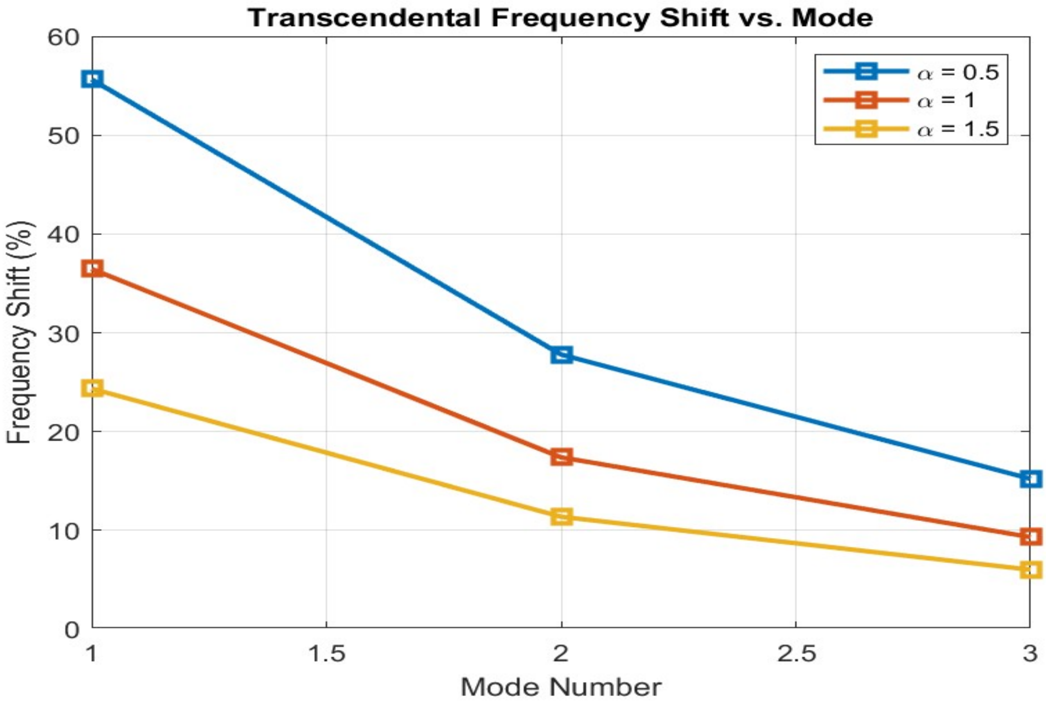

Figure 5.14 Frequency Shift due to add mass in analytical model

The result from simulation and analytical method showed that attaching mass leads to notable frequency reduction across all mode and tapered ratio. For α = 0.5 the simulation frequency decreased up to 60% for first mode, where for mode 2 and 3 are 31%, 20% decreased respectively as shown in figure 5.13. The corresponding transcendental results reveal shifts of 56%, 28%, and 15% Similarly, at α = 1 the shifts are approximately 37%, 21%, and 15% for the simulation data and 36%, 17%, and 9% for the transcendental data, and for α = 1.5 the frequency shifts are 23%, 15%, and 11% (simulation) compared to 24%, 11%, and 6% (transcendental) as shown in figure 5.14. This analysis confirms that the attached mass systematically lowers the natural frequencies.

5.5 Effect of tapered ratio on Natural Frequency

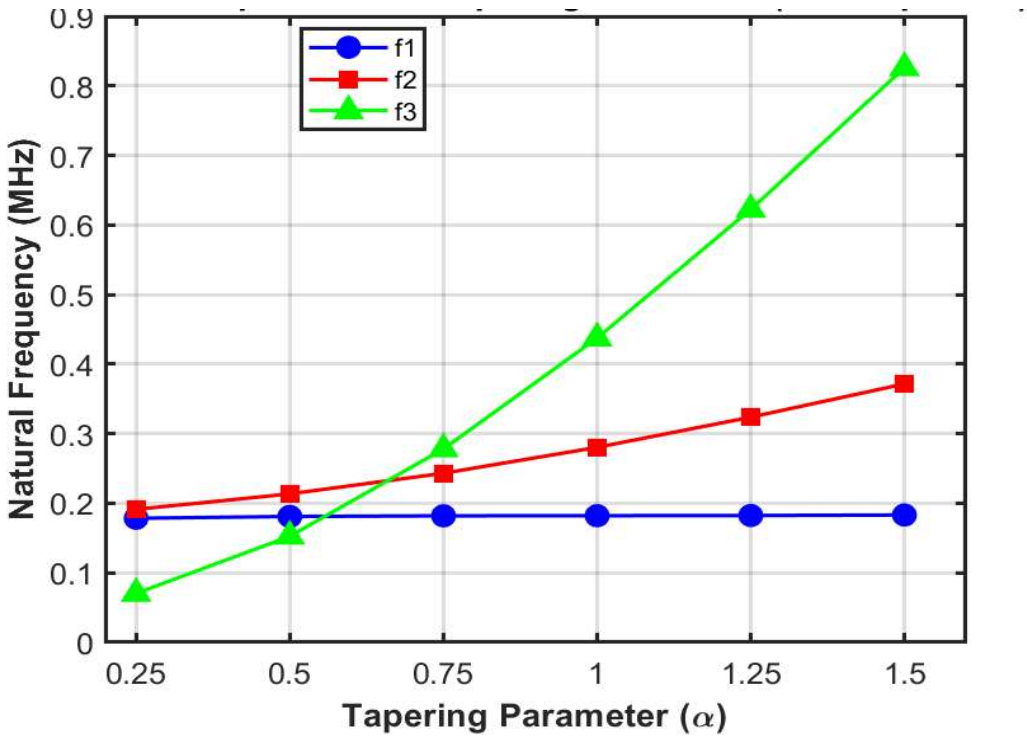

Figure 5.15 Effect of tapered ratio on Natural Frequency of micro-beam

Tapering significantly affects the natural frequency of acircular tapered cantilever micro-beam as shown in above figure 5.15 by altering its mass distribution and stiffness. As the tapering ratio increases, the beams cross-section reduces along its length, leading to a decrease in mass and an increase in stiffness, which generally results in a higher natural frequency.

5.6 Effect of tapered ratio on Modal Mass

In figure 5.18 x-axis represent the tapered ratio, which is linearly variational along the cross section.y-axis represent generalized mass. As values of tapered ratio increase the generalized mass for each mode changes. In both case with or without attached mass.

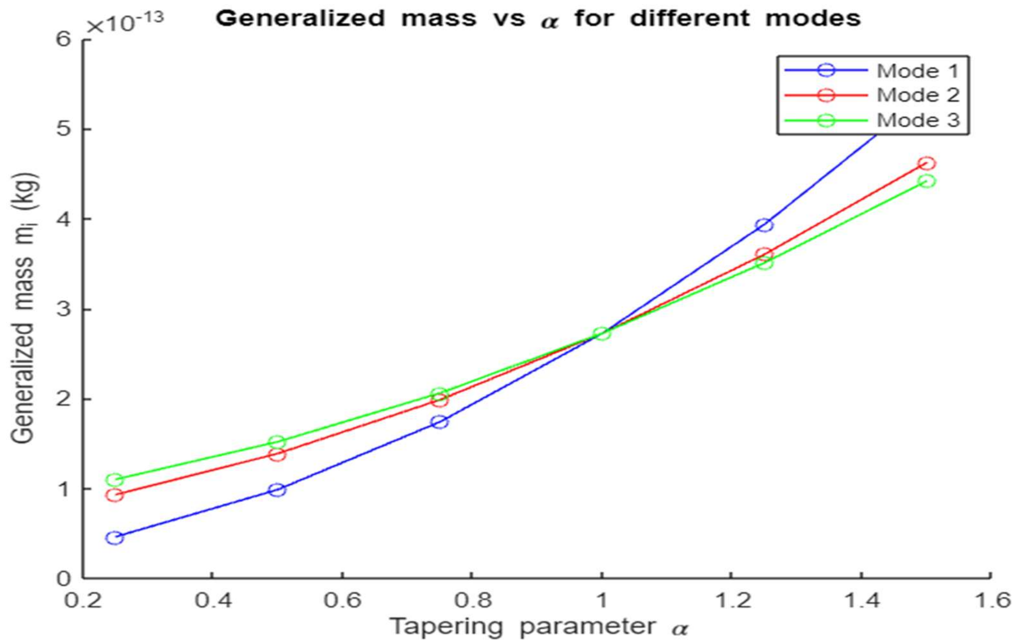

Figure 5.16 Effect of tapered ratio on Modal mass of micro-beam

5.7 Effect of tapered ratio on Modal Stiffness

In Figure 5.19 x-axis represent the tapered ratio, which is linearly variational along the cross section. y-axis represent generalized Stiffness. As values of tapered ratio increase the generalized Stiffness for each mode changes. In both case with or without attached mass.

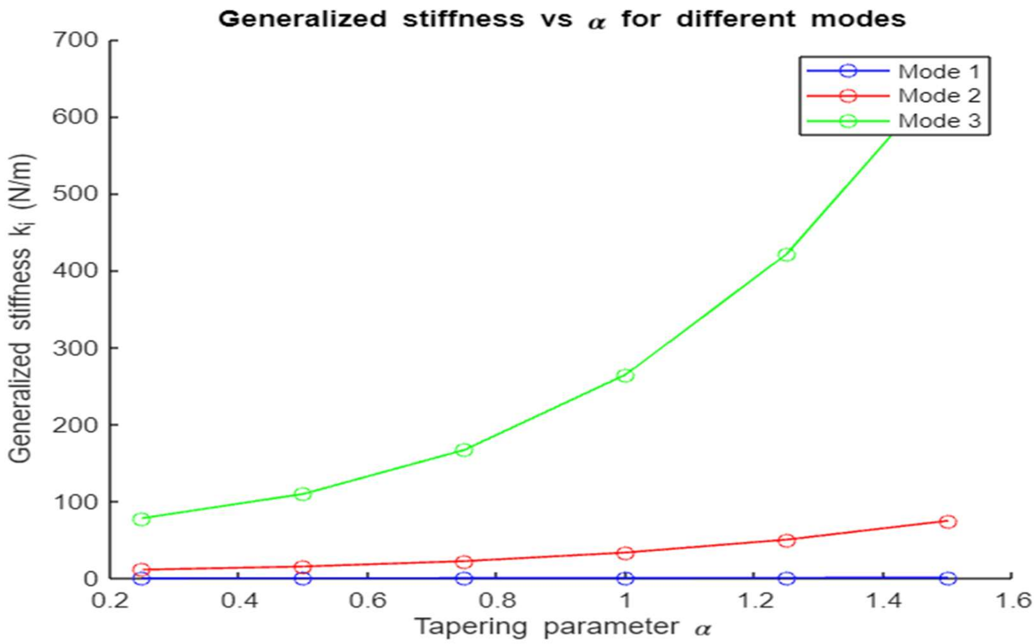

Figure 5.17 Effect of tapered ratio on Modal stiffness of micro-beam

CHAPTER SIX : CONCLUSION AND RECOMMENDATION

6.1 Conclusion

The equation of motion was derived using Lagrange equation and Hamilton principle. The research then investigated the free vibration analysis of the of circular tapered cantilever micro-beams used in MEMS device. Both Analytical and simulation method were used to study the effect of different tapering ratio and attached mass. This research found that the significant influence of tapering ratio on natural frequency, where increased tapering enhances stiffness and reduced mass distribution, leading to higher natural frequencies. The analytical and simulation results demonstrated close agreement, with deviations under 9.3 % for beam without an attached mass and up to 14.3 % for beam with a tip mass at end. The attached mass reduced the frequency for all three modes. The result obtained from analytical approaches using transcendental mode shapes were validated with Ansys simulations.

6.2 Recommendation

- Nonlinear Dynamics and Forced Vibrations: In order to apply to real world situation this study needs to expand nonlinear vibration regimes, like large amplitude vibration and forced excitation.
- Experimental validations: Physical experiments need to perform to validate analytical and simulation results.
- Environmental Factors: This study needs to investigate environmental factors such as effects of temperature, humidity, and damping to enable practical relevance.
- Higher-Order Modes and Rotational Effects: Requirements to explore higher vibrational modes and rotational inertia effect for rotating MEMS device. Advanced Geometries and Materials: Explore the microbeam with hexagonal structure or functionally graded materials.

REFERENCES

Abdel-Jaber, M., Al-Qaisia, A. A., & Abdel-Jaber, M. S. (2009). NONLINEAR NATURAL FREQUENCIES OF A TAPERED CANTILEVER BEAM. In Advanced Steel Construction (Vol. 5, Issue 3). www.hkisc.org

Abdel-Jaber, M. S., Al-Qaisia, A. A., Abdel-Jaber, M., & Beale, R. G. (2008). Nonlinear natural frequencies of an elastically restrained tapered beam. Journal of Sound and Vibration, 313(3–5), 772–783. https://doi.org/10.1016/j.jsv.2007.11.050

Aghamohammadi, M., Sorokin, V., & Mace, B. (2023). Nonlinear dynamics of parametrically excited cantilever beams with a tip mass considering nonlinear inertia and Duffing-type nonlinearity. Nonlinear Dynamics, 111(8), 7251–7269. https://doi.org/10.1007/s11071-023-08236-w

Akgöz, B., & Civalek, Ö. (2013). Free vibration analysis of axially functionally graded tapered Bernoulli-Euler microbeams based on the modified couple stress theory. Composite Structures, 98, 314–322. https://doi.org/10.1016/j.compstruct.2012.11.020

Attarnejad, R., Shahba, A., & Eslaminia, M. (2011). Dynamic basic displacement functions for free vibration analysis of tapered beams. JVC/Journal of Vibration and Control, 17(14), 2222–2238. https://doi.org/10.1177/1077546310396430

Attia, M. A., & Mohamed, S. A. (2022). Thermal vibration characteristics of pre/post-buckled bi-directional functionally graded tapered microbeams based on modified couple stress Reddy beam theory. Engineering with Computers, 38(3), 2079–2105. https://doi.org/10.1007/s00366-020-01188-4

Banerjee, J. R., Su, H., & Jackson, D. R. (2006). Free vibration of rotating tapered beams using the dynamic stiffness method. Journal of Sound and Vibration, 298(4–5), 1034–1054. https://doi.org/10.1016/j.jsv.2006.06.040

Bouchaala, A., Nayfeh, A. H., & Younis, M. I. (2016a). Frequency Shifts of Micro and Nano Cantilever Beam Resonators Due to Added Masses. Journal of Dynamic Systems, Measurement and Control, Transactions of the ASME, 138(9). https://doi.org/10.1115/1.4033075

Bouchaala, A., Nayfeh, A. H., & Younis, M. I. (2016b). THE EFFECT OF AN ADDED MASS ON THE FREQUENCY SHIFTS OF A CLAMPED-CLAMPED MICROBEAM FOR BIO-MASS DETECTION. http://proceedings.asmedigitalcollection.asme.org/pdfaccess.ashx?url=/data/conferences/asmep/90698/

Chhantyal, B., Adhikari, M., Chaudhary, B. B., & Luintel, M. C. (2024). Use of Polynomial Mode Shape Function in Free Vibration Analysis of Cantilever Pelton Turbine. Kathford Journal of Engineering and Management, 4(1), 92–101. https://kathford.edu.np/Journal/

Friswell, M. I., Ali, S. F., Bilgen, O., Adhikari, S., Lees, A. W., & Litak, G. (2012). Non-linear piezoelectric vibration energy harvesting from a vertical cantilever beam with tip mass. Journal of Intelligent Material Systems and Structures, 23(13), 1505–1521. https://doi.org/10.1177/1045389X12455722

Gao, R., Huang, Y., Wen, X., Zhao, J., & Liu, S. (2017a). Method to Further Improve Sensitivity for High-Order Vibration Mode Mass Sensors with Stepped Cantilevers. IEEE Sensors Journal, 17(14), 4405–4411. https://doi.org/10.1109/JSEN.2017.2712629

Gao, R., Huang, Y., Wen, X., Zhao, J., & Liu, S. (2017b). Method to Further Improve Sensitivity for High-Order Vibration Mode Mass Sensors with Stepped Cantilevers. IEEE Sensors Journal, 17(14), 4405–4411. https://doi.org/10.1109/JSEN.2017.2712629

Halvorsen, E., & Dong, T. (n.d.). ANALYSIS OF TAPERED BEAM PIEZOELECTRIC ENERGY HARVESTERS.

He, X., Li, D., Zhou, H., Hui, X., & Mu, X. (2021a). Theoretical and experimental studies on mems variable cross-section cantilever beam based piezoelectric vibration energy harvester. Micromachines, 12(7). https://doi.org/10.3390/mi12070772

He, X., Li, D., Zhou, H., Hui, X., & Mu, X. (2021b). Theoretical and experimental studies on mems variable cross-section cantilever beam based piezoelectric vibration energy harvester. Micromachines, 12(7). https://doi.org/10.3390/mi12070772

He, X., Li, D., Zhou, H., Hui, X., & Mu, X. (2021c). Theoretical and experimental studies on mems variable cross-section cantilever beam based piezoelectric vibration energy harvester. Micromachines, 12(7). https://doi.org/10.3390/mi12070772

Joshi, P., Kumar, S., Jain, V. K., Akhtar, J., & Singh, J. (2019). Distributed MEMS mass-sensor based on piezoelectric resonant micro-cantilevers. Journal of Microelectromechanical Systems, 28(3), 382–389. https://doi.org/10.1109/JMEMS.2019.2908879

Kim, P., Bae, S., & Seok, J. (2012). Resonant behaviors of a nonlinear cantilever beam with tip mass subject to an axial force and electrostatic excitation. International Journal of Mechanical Sciences, 64(1), 232–257. https://doi.org/10.1016/j.ijmecsci.2012.06.008

Li, Z., He, Y., Lei, J., Han, S., Guo, S., & Liu, D. (2019a). Experimental investigation on size-dependent higher-mode vibration of cantilever microbeams. Microsystem Technologies, 25(8), 3005–3015. https://doi.org/10.1007/s00542-018-4244-0

Li, Z., He, Y., Lei, J., Han, S., Guo, S., & Liu, D. (2019b). Experimental investigation on size-dependent higher-mode vibration of cantilever microbeams. Microsystem Technologies, 25(8), 3005–3015. https://doi.org/10.1007/s00542-018-4244-0

Luintel, M. C. (2021). Development of Polynomial Mode Shape Functions for Continuous Shafts with Different End Conditions. Journal of the Institute of Engineering, 16(1).

Luintel, M. C. (2024). Textbook of Mechanical Vibrations. https://doi.org/https://doi.org/10.1007/978-981-99-3614-4_1

M. Lajimi∗ Amir, & Amir M. Lajimi∗, E. A.-R., G. R. H. ‡. (2009). On Natural Frequencies and Mode Shapes of Microbeams. News wood Ltd.: International Association of Engineers.

Maharjan, S., & Luintel, M. C. (2025). Harmonic analysis of a Simply-Supported-Fixed-Beam of uniform cross-section with a concentrated mass and concentrated harmonic force at mid-span using Numerical Simulation. Journal of the Institute of Engineering, 18(1).

Meesala, V. C., Hajj, M. R., Ragab, S. A., & Shahab, S. (2018). Modeling And Analysis Of A Cantilever Beam Tip Mass System.

Nirmall T, & Vimala S. (2013). Volume 5 Issue 4, April 2016 www.ijsr.net Licensed Under Creative Commons Attribution CC BY Free Vibration Analysis of Cantilever Beam of Different Materials. In International Journal of Science and Research (IJSR) ISSN. www.ijsr.net

Ojha, K., & Luintel, M. C. (n.d.). Proceedings of 14 th IOE Graduate Conference Free Vibration Analysis of Multidisc Cantilever Shaft System.

Pallay, M., & Towfighian, S. (2017). Parametrically excited electrostatic MEMS cantilever beam with flexible support. Journal of Vibration and Acoustics, 139(2). https://doi.org/10.1115/1.4034954

Parsediya, D. K., Singh, J., & Kankar, P. K. (2015). Variable width based stepped MEMS cantilevers for micro or pico level biosensing and effective switching. Journal of Mechanical Science and Technology, 29(11), 4823–4832. https://doi.org/10.1007/s12206-015-1029-6

Rahmani, A., Babaei, A., & Faroughi, S. (2020). Vibration characteristics of functionally graded micro-beam carrying an attached mass. Mechanics of Advanced Composite Structures, 7(1), 49–58. https://doi.org/10.22075/macs.2019.18186.1214

Rao, S. S. . (2011). Mechanical vibrations. Prentice Hall.

Sadrehaghighi, I. (n.d.). CFD Open Series Patch Mesh Generation in CFD A N N A P O L I S , MD Cyliner Head-(Polyhedral cells) Mixer (SAMM cells) Typical Turbo-Machine Mesh (Hexahedral cells) Wing-Body-Pylon-Nacelle (Tetrahedral cells).

Schultz, J. A., Heinrich, S. M., Josse, F., Dufour, I., Nigro, N. J., Beardslee, L. A., & Brand, O. (2015). Lateral-Mode Vibration of Microcantilever-Based Sensors in Viscous Fluids Using Timoshenko Beam Theory. Journal of Microelectromechanical Systems, 24(4), 848–860. https://doi.org/10.1109/JMEMS.2014.2354596

Singh, S. S., Pal, P., & Pandey, A. K. (2016). Mass Sensitivity of Nonuniform Microcantilever Beams. Journal of Vibration and Acoustics, 138(6). https://doi.org/10.1115/1.4034079

Sun, W., Sun, Y., Yu, Y., & Zheng, S. (2016). Nonlinear vibration analysis of a type of tapered cantilever beams by using an analytical approximate method.

Structural Engineering and Mechanics, 59(1), 1–14. https://doi.org/10.12989/sem.2016.59.1.001

Wang, Z., & Li, R. (2018). Transverse Vibration of Rotating Tapered Cantilever Beam with Hollow Circular Cross-Section. Shock and Vibration, 2018. https://doi.org/10.1155/2018/1056397

Wong, F. T., Gunawan, J., Agusta, K., Herryanto, H., & Tanaya, L. S. (2019). On the Derivation of Exact Solutions of a Tapered Cantilever Timoshenko Beam. Civil Engineering Dimension, 21(2), 89–96. https://doi.org/10.9744/ced.21.2.89-96

Yaylı, M. Ö., Kandemir, S. Y., & Çerçevik, A. E. (2016). 2106. A practical method for calculating eigenfrequencies of a cantilever microbeam with the attached tip mass. Journal of Vibroengineering, 18(5), 3070–3077. https://doi.org/10.21595/jve.2016.16636

APPENDIX

Code for analytical Solution

```
% Define beam parameters
L = 100e-6; % Length in meters (100 μm)
R0 = 1.22e-6; % Radius at fixed end in meters (1.22 μm)
rho = 2330; % Density in kg/m^3
E = 160e9; % Young's modulus in Pa (160 Gpa)
M = 0.4e-12; % Tip mass in kg (0.4×10^-12 kg)
alpha values = [0.25, 0.5, 0.75, 1, 1.25, 1.5]; % Tapering parameters
% Constants for mode shapes (β_iL for uniform beam)
betaL = [1.8751, 4.6941, 7.8548]; % Approximate eigenvalues for modes 1, 2, 3
phiL = [1, 0.56, 0.38]; % Approximate mode shape values at x=L
% Reallocate results matrix
results = [];
% Numerical integration setup
x = Lin space (0, L, 1000); % Discretize beam length for integration
for alpha = alpha values
 % Tapering functions
 radius = @(x) R0 * (1 + (alpha - 1) * (x / L)); % Linear tapering of radius
 area = @(x) pi * radius(x). ^2; % Cross-sectional area
 I = @(x) pi * radius(x). ^4 / 4; % Moment of inertia
 % Compute beam mass for uniform case (alpha = 1) as reference
 m_beam_uniform = pi * rho * R0^2 * L;
 % Mode shape function (simplified for uniform beam, adjusted later)
 for i = 1:3 % Modes 1, 2, 3
 beta = betaL(i) / L;% β_i for mode i
 % Mode shape (transcendental form)
 phi = @(x) (cosh(beta * x) - cos(beta * x) - ...
 (cosh(beta * L) + cos(beta * L)) / (sinh(beta * L) + sin(beta * L)) * ...
 (sinh(beta * x) - sin(beta * x)))
 % Evaluate mode shape over x
 phi_x = arrayfun(phi, x);
    % Normalize mode shape so max|φ(x)| = 1
```

```
 max_phi = max(abs(phi_x));
 phi_x = phi_x / max_phi;
 Mi = max_phi; % Normalization constant (approximate)
 % Compute second derivative of mode shape numerically
 dx = x(2) - x(1);
 phi_xx = gradient(gradient(phi_x, dx), dx); % Second derivativ
 % Modal mass integral: m_i = πρR₀² ∫ [1 + (α-1)x/L]² φ_i² dx + M φ_i²(L)
 mass_integrand = pi * rho * R0^2 * (1 + (alpha - 1) * (x / L)).^2 .* phi_x.^2;
 m_i_distributed = trapz(x, mass_integrand); % Numerical integration
 m_i = m_i_distributed + M * phiL(i)^2; % Add tip mass contribution
 % Modal stiffness integral: k_i = (π/4) E R₀⁴ ∫ [1 + (α-1)x/L]⁴ [φ_i''(x)]² dx
 stiffness_integrand = (pi / 4) * E * R0^4 * (1 + (alpha - 1) * (x / L)).^4 .* phi_xx.^2;
 k_i = trapz(x, stiffness_integrand); % Numerical integration
 % Natural frequency
 omega_i = sqrt(k_i / m_i); % Circular frequency in rad/s
 f_i = omega_i / (2 * pi) / 1e6; % Frequency in MHz
 % Store results
 results = [results; alpha, i, m_i, k_i, f_i];
 end
end
% --- Plotting ---
% Plot m_i vs alpha
figure(1);
hold on;
colors = ['b', 'r', 'g'];
for i = 1:3
 indices = results(:, 2) == i;
 plot(results(indices, 1), results(indices, 3), [colors(i) '-o'], 'DisplayName', ['Mode '
num2str(i)]);
end
xlabel('Tapering Parameter \alpha');
ylabel('Modal Mass m_i (kg)');
title('Modal Mass vs \alpha');
```

```
legend('Location','northoutside','Orientation','horizontal');
hold off;
% Plot k_i vs alpha
figure(2);
hold on;
for i = 1:3
 indices = results(:, 2) == i;
 plot(results(indices, 1), results(indices, 4), [colors(i) '-o'], 'DisplayName', ['Mode '
num2str(i)]);
end
xlabel('Tapering Parameter \alpha');
ylabel('Modal Stiffness k_i (N/m)');
title('Modal Stiffness vs \alpha');
legend('show');
hold off;
% Plot f_i vs alpha
figure(3);
hold on;
for i = 1:3
 indices = results(:, 2) == i;
 plot(results(indices, 1), results(indices, 5), [colors(i) '-o'], 'DisplayName', ['Mode '
num2str(i)]);
end
xlabel('Tapering Parameter \alpha');
ylabel('Natural Frequency f_i (MHz)');
title('Natural Frequency vs \alpha');
legend('Location','northoutside','Orientation','horizontal');
hold off;
% --- Save to Excel ---
T = array2table(results, 'VariableNames', {'Alpha', 'Mode', 'm_i', 'k_i', 'f_i'});
writetable(T, 'tapered_modal_parameters.xlsx');
% Display results for verification
disp('Alpha Mode m_i (kg) k_i (N/m) f_i (MHz)');
```

```
for i = 1:size(results, 1)
 fprintf('%.2f %d %.3e %.2f %.3f\n', results(i, 1), results(i, 2), ...
 results(i, 3), results(i, 4), results(i, 5));
end
% Plot the normalized mode shapes (x in nondimensional units)
x_plot = linspace(0, 1, 1000);
figure;
subplot(3, 1, 1);
plot(x_plot, phi1(x_plot), 'b', 'LineWidth', 2);
xlabel('x (nondimensional)'); ylabel('\phi_1(x)');
title('Normalized Mode Shape for Mode 1');
grid on;
subplot(3, 1, 2);
plot(x_plot, phi2(x_plot), 'r', 'LineWidth', 2);
xlabel('x (nondimensional)'); ylabel('\phi_2(x)');
title('Normalized Mode Shape for Mode 2');
grid on;
subplot(3, 1, 3);
plot(x_plot, phi3(x_plot), 'g', 'LineWidth', 2);
xlabel('x (nondimensional)'); ylabel('\phi_3(x)');
title('Normalized Mode Shape for Mode 3');
grid on;
```

Dhan Bahadur Saud

Free vibration analysis of circular tapered microbeam

Tribhuvan University

Document Details

Submission ID

trn:oid:::3117:447260179

Submission Date

Apr 9, 2025, 11:26 AM GMT+5:45

Download Date

Apr 9, 2025, 11:29 AM GMT+5:45

File Name

Dhan Bahadur Saud.pdf

File Size

2.3 MB

33 Pages

7,286 Words

38,051 Characters

6% Overall Similarity

The combined total of all matches, including overlapping sources, for each database.

Filtered from the Report

- Bibliography
- Quoted Text
- Cited Text
- Small Matches (less than 8 words)

Match Groups

- **47** Not Cited or Quoted 6%
  Matches with neither in-text citation nor quotation marks
- **0** Missing Quotations 0%
  Matches that are still very similar to source material
- **0** Missing Citation 0%
  Matches that have quotation marks, but no in-text citation
- **0** Cited and Quoted 0%
  Matches with in-text citation present, but no quotation marks

Top Sources

- 4% Internet sources
- 4% Publications
- 0% Submitted works (Student Papers)

Integrity Flags

1 Integrity Flag for Review

Replaced Characters
13 suspect characters on 7 pages
Letters are swapped with similar characters from another alphabet.

Our system's algorithms look deeply at a document for any inconsistencies that would set it apart from a normal submission. If we notice something strange, we flag it for you to review.

A Flag is not necessarily an indicator of a problem. However, we'd recommend you focus your attention there for further review.

Match Groups

- **47** Not Cited or Quoted 6%
  Matches with neither in-text citation nor quotation marks
- **0** Missing Quotations 0%
  Matches that are still very similar to source material
- **0** Missing Citation 0%
  Matches that have quotation marks, but no in-text citation
- **0** Cited and Quoted 0%
  Matches with in-text citation present, but no quotation marks

Top Sources

4% Internet sources
4% Publications
0% Submitted works (Student Papers)

Top Sources

The sources with the highest number of matches within the submission. Overlapping sources will not be displayed.

1	Publication	Mahesh Chandra Luintel. "Textbook of Mechanical Vibrations", Springer Science a...	1%
2	Internet	shellbuckling.com	<1%
3	Internet	edoc.tips	<1%
4	Publication	Naotake Noda, Richard B. Hetnarski, Yoshinobu Tanigawa. "Thermal Stresses", C...	<1%
5	Publication	Dafeng Tang, C. W. Lim, Ling Hong, Jun Jiang, S. K. Lai. "Dynamic Response and St...	<1%
6	Publication	Srinivasan Gopalakrishnan. "Wave Propagation in Materials and Structures", CRC ...	<1%
7	Internet	elibrary.tucl.edu.np	<1%
8	Internet	researchspace.ukzn.ac.za	<1%
9	Internet	p.pdfhall.com	<1%
10	Internet	catalog.lib.kyushu-u.ac.jp	<1%

11 Internet

pepite-depot.univ-lille.fr <1%

12 Internet

repositorio.comillas.edu <1%

13 Internet

uhra.herts.ac.uk <1%

14 Internet

go.griffith.ie <1%

15 Internet

open.metu.edu.tr <1%

16 Internet

www.bioforce.uni-tuebingen.de <1%

17 Publication

Choi, M.. "Vibration analysis of a dummy fuel rod continuously supported by spac... <1%

18 Publication

Goodson, M.. "Simulation of coalescence and breakage: an assessment of two sto... <1%

19 Publication

Noriaki Ishii, Keiko Anami, Charles W. Knisely. "chapter 2 Vibrations", IGI Global, ... <1%

20 Internet

www.mdpi.com <1%

21 Publication

Bekir Akgöz, Ömer Civalek. "Buckling analysis of functionally graded microbeams... <1%

22 Publication

Chen, Y., J. Zhang, and H. Zhang. "Flapwise bending vibration of rotating tapered ... <1%

23 Publication

Nikoli, A., and S. alini. "A rigid multibody method for free vibration analysis of be... <1%

24 Publication

Panchal, Mitesh B., S.H. Upadhyay, and S.P. Harsha. "Vibrational characteristics of... <1%

25 Publication

Vepa. "Fundamentals of Structural Control", Dynamics of Smart Structures, 04/23... <1%

26 Internet

ir-library.mmust.ac.ke <1%

27 Internet

sanad.iau.ir <1%

ACCEPTED PAPER

[jie] Editor Decision

TUTA-PCU <tuta@pcampus.edu.np>

Wed, Apr 2, 10:18 AM (8 days ago)

Dhan Bahadur Saud:

We have reached a decision regarding your submission to Journal of the Institute of Engineering, "Free Vibration Analysis of Circular Tapered Cantilever Micro-beams".

Our decision is to: Accept Submission

Journal of the Institute of Engineering